Perirhinal and Parahippocampal Cortices of the Macaque Monkey: Cortical Afferents

WENDY A. SUZUKI AND DAVID G. AMARAL
Laboratory of Neuropsychology, NIMH, Bethesda, Maryland 20892 (W.A.S.); Center for
Behavioral Neuroscience, SUNY at Stony Brook, Stony Brook, New York 11794-2575 (D.G.A.)

ABSTRACT

Neuropsychological studies have recently demonstrated that the macaque monkey perirhinal (areas 35 and 36) and parahippocampal (areas TH and TF) cortices contribute importantly to normal memory function. Unfortunately, neuroanatomical information concerning the cytoarchitectonic organization and extrinsic connectivity of these cortical regions is meager. We investigated the organization of cortical inputs to the macaque monkey perirhinal and parahippocampal cortices by placing discrete injections of the retrograde tracers fast blue, diamidino yellow, and wheat germ agglutinin conjugated to horseradish peroxidase throughout these areas. We found that the macaque monkey perirhinal and parahippocampal cortices receive different complements of cortical inputs. The major cortical inputs to the perirhinal cortex arise from the unimodal visual areas TE and rostral TEO and from area TF of the parahippocampal cortex. The perirhinal cortex also receives projections from the dysgranular and granular subdivisions of the insular cortex and from area 13 of the orbitofrontal cortex. In contrast, area TF of the parahippocampal cortex receives its strongest input from more caudal visual areas V4, TEO, and caudal TE, as well as prominent inputs from polymodal association cortices, including the retrosplenial cortex and the dorsal bank of the superior temporal sulcus. Area TF also receives projections from areas 7a and LIP of the posterior parietal lobe, insular cortex, and areas 46, 13, 45, and 9 of the frontal lobe. As with area TF, area TH receives substantial projections from the retrosplenial cortex as well as moderate projections from the dorsal bank of the superior temporal sulcus; unlike area TF, area TH receives almost no innervation from areas TE and TEO. It does, however, receive relatively strong inputs from auditory association areas on the convexity of the superior temporal gyrus. © 1994 Wiley-Liss, Inc.

Key words: hippocampal formation, memory, entorhinal cortex, polysensory cortex, medial temporal lobe

The elegant studies of the well-known amnesic patient, H.M., by Milner and colleagues (Scoville and Milner, 1957; Milner et al., 1968; Corkin, 1984) first identified the structures of the medial temporal lobe as critical for normal memory function. Recent clinicopathological analyses of human amnesic cases (Zola-Morgan et al., 1986; Victor and Agamanolis, 1990) as well as experimental studies in the macaque monkey (Zola-Morgan and Squire, 1986, 1993) and the rat (Morris et al., 1982; Jarrard, 1993) have confirmed the long-held belief that the hippocampal formation, including the dentate gyrus, hippocampus proper, subicular complex, and entorhinal cortex, is an important component of the medial-temporal lobe memory system. Over the last few years, however, views concerning which other structures should be included within the medial-temporal lobe memory system have undergone substantial revision. It is now clear, for example, that the amygdaloid complex, once thought to contribute along with the hippo-campal formation to normal memory function (Mishkin,

1978), has little or no role in recognition memory function as assayed by the delayed nonmatching-to-sample task (Zola-Morgan et al., 1989a). In contrast, attention has recently been focused on the perirhinal and parahippocampal cortices, areas that had not previously been implicated in memory function.

There are both behavioral and neuroanatomical data supporting the idea that the macaque monkey perirhinal and parahippocampal cortices contribute importantly to normal memory function. For example, it has recently been shown that selective damage to these areas produces severe and long-lasting memory impairments in both the visual and tactual modalities (Zola-Morgan et al., 1989b; Suzuki et

al., 1993). Similarly, bilateral conjoint lesions of the entorhinal and perirhinal cortices in the macaque monkey (Gaffan and Murray, 1992) or the rat (Otto and Eichenbaum, 1992; Mumby and Pinel, 1994) produce significant memory impairments. From a neuroanatomical perspective, the perirhinal and parahippocampal cortices are strongly associated with the hippocampal formation. Insausti et al. (1987) found that the macaque monkey perirhinal and parahippocampal cortices provide approximately two-thirds of the direct cortical input to the entorhinal cortex. The perirhinal and parahippocampal cortices also receive an equally robust return projection from the entorhinal cortex (Suzuki and Amaral, 1994a). Although a growing body of evidence supports the idea that the perirhinal and parahippocampal cortices contribute importantly to normal memory function, relatively little is known about the neuroanatomical organization of these areas. In particular, there has been no comprehensive analysis of the origin of cortical inputs to the perirhinal and parahippocampal regions.

Jones and Powell (1970), in their seminal paper on converging sensory pathways within the macaque monkey cortex, were the first to indicate that the perirhinal and parahippocampal cortices are higher order polymodal associational areas. In a series of anterograde degeneration studies, the authors demonstrated that the perirhinal and parahippocampal cortices receive convergent sensory information from higher order unimodal visual, auditory, and somatosensory cortical regions as well as from other polymodal association areas. Seltzer and Pandya (1976) confirmed that the parahippocampal cortex receives convergent projections from area 7 of the parietal lobe, from auditory association areas of the anteroventral STG, and from prestriate visual areas. Van Hoesen and colleagues (Van Hoesen and Pandya, 1975; Van Hoesen et al., 1975) provided further evidence for strong visual inputs to the macaque monkey perirhinal cortex and for projections from area 13 of the orbitofrontal cortex. More recently, Mesulam and Mufson (1982a,b) demonstrated that the insular cortex, much of which is related to somatosensory function, is reciprocally connected with the perirhinal cortex.

Although previous studies provided indications that the perirhinal and parahippocampal cortices receive a variety of neocortical inputs, one can never be certain, using anterograde tracing techniques alone, that all of their cortical inputs have been identified. Martin-Elkins and Horel (1992) recently published findings from two cases in macaque monkeys in which wheat germ agglutinin conjugated to horseradish peroxidase (WGA-HRP) injections were placed into area TF. Although these injections partially invaded adjacent cortical areas TE or TEO, the findings were suggestive that the origins of cortical projections to area TF were more widespread than previously appreciated.

In order to determine the full complement of cortical inputs to the macaque monkey perirhinal and parahippocampal cortices, we have undertaken a series of studies using sensitive retrograde tracing techniques. We produced relatively small, discrete injection sites in order to determine the topographical organization of cortical projections to the perirhinal and parahippocampal cortices; labeling resulting from 31 injections covering much of the rostrocaudal and mediolateral extents of these fields was analyzed. Moreover, in order to quantify the density of cortical labeling resulting from injections in the perirhinal or parahippocampal cortex, we plotted and counted individual, retrogradely labeled cells from sections spaced at 480 μm

intervals throughout the entire cortical mantle. To display the results of these analyses, we modified the two-dimensional, unfolded mapping technique of Van Essen and Maunsell (1980) to provide a quantitative representation of the magnitude of projections from large portions of the cerebral cortex. Analysis of these experiments with these techniques has provided a clear and quantitative picture of the full scope of cortical inputs to the macaque monkey perirhinal and parahippocampal cortices.

MATERIALS AND METHODS

Twenty *Macaca fascicularis* monkeys of either sex (weighing 3–5 kg at the time of surgery) were used in these studies. In one animal, a single injection of the retrograde tracer WGA-HRP (Sigma, St. Louis, MO) was placed in area TF. In the remaining 19 animals, an injection of the fluorescent retrograde tracer fast blue (FB; Dr. Illing GmbH and Co.) was placed at one site and a second tracer, diamidino yellow (DY; Dr. Illing GmbH and Co.), was placed at a different site located at least 2 mm rostral or caudal to the first site. Of the 39 attempted injections, 27 were located entirely within the confines of the perirhinal or parahippocampal cortices, and four were situated at or near the border of the parahippocampal cortex with adjacent areas TE, TEO, or V4. The location of the perirhinal and parahippocampal cortices in the macaque monkey brain is illustrated in Figure 1, and a straight-line, unfolded map of the temporal lobe is shown in Figure 2. The locations of the 31 injection sites are illustrated on an unfolded map of the entorhinal, perirhinal, and parahippocampal cortices in Figure 3B.

Surgical, injection, and histological procedures

For experiments conducted prior to August, 1990, animals were preanesthetized with ketamine hydrochloride (8 mg/kg,i.m.), followed by Nembutal (25 mg/kg, i.p.), and mounted in a Kopf stereotaxic apparatus. A venous catheter was placed, and Nembutal was supplemented as necessary throughout surgery. For the remaining experiments, animals were preanesthetized with ketamine hydrochloride (8 mg/kg, i.m.), intubated with a tracheal cannula, and mounted in a Kopf stereotaxic apparatus. The animals were then mechanically ventilated and brought to a surgical level of anesthesia with isoflurane. Using aseptic surgical procedures, the skull was exposed, a small burr hole was made at a site appropriate for the injection as determined from the atlas of Szabo and Cowan (1984), and the dura was reflected. In most cases, a tungsten microelectrode was lowered through the intended injection site, and extracellular unit responses were recorded. By determining electrophysiologically distinctive landmarks such as the pyramidal cell layer of the hippocampus, the ventricle, or the bottom of the brain, we were able to determine more precisely the appropriate dorsoventral coordinate for placement of the injection. In most cases, the tracer substances were dispensed through glass micropipettes using air-pressure pulses (Amaral and Price, 1983). Injections aimed at the rostral tip of the temporal pole, however (cases M-20-91, M-21-91, and M-22-91; Figure 3B), were made using a 1 μl Hamilton syringe. For the WGA-HRP injection, 50 nl of a 1% solution of WGA-HRP was dispensed at a rate of approximately 4 nl/minute. In the cases in which DY and FB were injected, between 500 and 1,500 nl of a 2% DY solution or between

500 and 650 nl of a 3% FB solution was dispensed. Both the FB and the DY solutions were dissolved in distilled water. The most common rate of injection for these cases was approximately 100 nl/minute. In all cases, at the termination of the injection, the pipette was raised 100 μm and left in place for an additional 10 minutes. The pipette was then slowly withdrawn over a period of approximately 20–30 minutes, and the dura was sutured. An analgesic (0.15 mg/kg of oxymorphone, 3 × daily for 2 days) was administered postsurgically, and a prophylactic regime of antibiotics (50 mg/kg of Claforan, 3 × daily) was administered during the first 5 days of the survival period.

In the cases with fluorescent retrograde tracer injections, following a 14-day survival period, animals were deeply anesthetized and perfused intracardially using one of two different perfusion protocols. For the "pH-shift perfusion protocol," the animals were first perfused with 500 ml of 0.9% saline solution, followed by 2,750 ml of a 0.1 M sodium acetate buffer with 4% paraformaldehyde (pH 6.0) at 4°C. The perfusion was completed by passing 3,000 ml of a 0.1 M sodium borate buffer with 4% paraformaldehyde (pH 9.5) at 4°C. The fixative solutions were perfused over a period of approximately 60 minutes. For the "modified immunohistochemistry perfusion protocol," perfusion was initiated with 1,000 ml of 1% paraformaldehyde in 0.1 M phosphate buffer (pH 7.2) followed by 7,500 ml of a 4% paraformaldehyde solution in 0.1 M phosphate buffer (pH 7.2), both at 4°C. These fixatives were perfused over a period of approximately 60 minutes.

In all cases, following the perfusion, the calvarium was removed and the brain exposed. The animal's head was then remounted in the Kopf stereotaxic apparatus and the brain was "blocked" in the coronal plane at two rostrocaudal locations; a scalpel blade mounted to an electrode carrier was moved from the left lateral surface of the brain to the right in a sawing fashion to effect the blocking. The first cut was typically made at AP +28, just rostral to the temporal poles, and the second cut was typically made at AP −2 at a level just caudal to the caudal pole of the hippocampus. The brain was then removed from the skull, sectioning of the blocks was completed, and individual blocks were postfixed for 6 hours in either the 0.1 M borate fixative or the 4%-paraformaldehyde fixative depending on whether the "pH-shift" or the "modified immunohistochemistry" perfusion protocol, respectively, was used. The brains were then cryoprotected first in a 10% and then in a 20% glycerol solution in 0.1 M phosphate buffer (pH 7.4) containing 2% dimethylsulfoxide for 1 and 3 days, respectively. All brains were sectioned at 30 μm on a freezing, sliding microtome.

For analysis of the retrogradely labeled cells resulting from the fluorescent tracer injections, two adjacent series of sections were immediately mounted on slides and stored, desiccated at −20°C, until analyzed. All analysis was done using a Leitz Dialux-20 microscope equipped for fluorescence microscopy. An adjacent series of sections was stained with thionin to allow for determination of cytoarchitectonic boundaries.

For the case with an injection of WGA-HRP, the survival period was 48 hours, and the animal was then deeply anesthetized and perfused intracardially, first with 1% paraformaldehyde in a 0.9% saline solution, then with a 4% paraformaldehyde in a 0.1 M phosphate buffer solution (pH 7.4). Processing of this brain was carried out as described previously (Insausti et al., 1987).

Analysis of the distribution of retrogradely labeled cells

The distribution of retrogradely labeled cells was analyzed using a computer-aided X-Y plotting system (Minnesota Datametrics MD-2 digitizer and software). In all cases, the position of each retrogradely labeled cell was plotted for every section in a 1-in-16 series (i.e., spaced every 480 μm) throughout the entire brain.

Construction of two-dimensional, unfolded density maps

An appreciation of the topographical organization of the cortical inputs to the perirhinal and parahippocampal cortices is greatly facilitated if the distribution of labeled cells is represented on two-dimensional, unfolded maps of the neocortex. Figure 2D illustrates a straight-line, unfolded, two-dimensional map of the temporal lobe of a macaque monkey brain. Coronal sections from four rostrocaudal levels through the map are also illustrated to show the relationship of the unfolded map to standard coronal sections. Figure 2A–C shows line drawings of a ventral, lateral, and frontal view, respectively, of the macaque monkey brain indicating how the unfolded map relates to the gross surface landmarks of the brain. In order to construct these unfolded maps, line drawings of layer IV of the cortex from a series of Nissl-stained sections sampled at 480-μm intervals were drawn at a magnification of ×13 with a Nikon stereomicroscope. The boundaries of the major cortical areas and major sulci were determined microscopically and marked on the line drawings. The sections were then "unfolded" onto a series of equally spaced straight lines essentially according to the procedures outlined by Van Essen and Maunsell (1980). Sections from rostral levels were aligned along the fundus of the rhinal sulcus, whereas those from caudal levels were aligned along the distal border of the subicular complex.

Density maps of the temporal lobe

Figures 5, 9D, 11, 12, and 16D show a series of unfolded, two-dimensional density maps of the macaque monkey temporal lobe. These maps quantitatively illustrate the density of retrogradely labeled cells observed throughout the temporal lobe. A detailed description of the method used to construct these density maps is given in Suzuki and Amaral (1994b). Briefly, MD-2 plot files containing the section outlines and distribution of retrogradely labeled cells were printed at a magnification of ×13. Using a Nikon stereomicroscope, layer IV of the cortex as well as the major cortical and sulcal landmarks were microscopically determined and marked onto the section outlines. Layer IV of each section was then divided into 769-μm-wide segments (10-mm-wide segments on the ×13 magnification plotted sections) forming contiguous 769-μm-wide "columns" of cortex. The number of cells in each column of cortex throughout all regions of the temporal lobe except the entorhinal cortex was counted, and the cortical landmarks, along with the cell count data, were superimposed onto the straight-line, unfolded map for that case.

Figure 4 shows a representative histogram indicating the number of occurrences (Y-axis) of retrogradely labeled cells per column of cortex throughout the temporal lobe in case M-3-90 FB. The shape of the curve was very similar for cases with injections of DY. Because the raw cell-count data on the unfolded maps did not provide a visual means of

appreciating the density of labeled cells, we attempted to translate the cell-count data into different gray levels. How to assign the range of cell-density counts to different gray levels, however, was not immediately obvious and necessitated an empirical process. Given the exponential nature of the distribution of labeled cells (Fig. 4), it was clear that defining different density levels with a simple arithmetic division was not appropriate (i.e., taking the highest number of cells per cortical column and dividing by four). Similarly, a parcelling based on absolute density levels did not seem appropriate because of the natural variation in the number of labeled cells depending on the size and location of the different injection sites. Moreover, the density of retrogradely labeled cells in the cases containing DY injections was consistently lower than the total number of retrogradely labeled cells observed after injections of FB. Thus, we "normalized" the cell-density data across cases using a percentile algorithm. For each case, the number of cells per column of cortex throughout the temporal lobe was entered into a database (Microsoft Excel), and the counts that fell within the 91st to 100th percentiles were designated as the highest density level and were shown in black (or in red on the color maps). The counts that fell between the 71st and the 90th percentiles were designated the next highest density level and were shown in dark gray (or in yellow on the color maps). Those between the 41st and the 70th percentiles were shown in the next lightest shade of gray (or in green on the color maps), and, finally, those counts that fell between the 1st and the 40th percentiles were shown in the lightest shade of gray (or in blue on the color maps). So, for example, in experiment M-3-90 FB, the red voxels in the unfolded density maps in Figure 9 (see also Fig. 4) represent the highest density level and correspond to columns of cortex containing between 94 and 286 cells (i.e., 91st to 100th percentiles). The yellow voxels represent the next highest density level and correspond to columns of cortex containing between 31 and 93 cells (71st to 90th percentiles). The voxels shown in green correspond to columns of cortex containing between seven and 30 cells (41st to 70th percentiles) and the voxels shown in the blue represent between one and six labeled cells per column of cortex (1st to 40th percentiles). Although this strategy is somewhat arbitrary, it appeared to provide the most reasonable and consistent representation of the gradients of retrogradely labeled cell density throughout the temporal lobe in all cases.

The ranges of labeled cells per column of cortex representing the 100th, 90th, 70th, and 40th percentiles for the subset of 17 cases analyzed in this way were as follows: range for 100th percentile, 139–498 cells; range for 90th percentile, 36–129 cells; range for 70th percentile, 9–38 cells; range for 40th percentile, 3–8 cells.

Description of Table 1

In order to provide a more quantitative assessment of the magnitude of cortical projections to the perirhinal and parahippocampal cortices, we have calculated the percentage of labeled cells observed in various cortical areas throughout the brain in representative cases with injections in area 36, area TF, and area TH (Table 1). Thus, for each case, the number of retrogradely labeled cells observed in various cortical areas throughout the temporal lobe, frontal lobe, insular cortex, cingulate and retrosplenial cortices, as well as the posterior parietal cortex was calculated. This number was then divided by the total number of

cortical-labeled cells observed outside the area of injection to compute the percentages shown in Table 1. In case M-3-90 FB, for example, we plotted a total of 42,275 labeled cells outside the perirhinal cortex. In cases M-2-90 FB and M-3-91 FB, we plotted 13,782 and 18,234 labeled cells, respectively, outside the area of injection.

We would like to point out that, although the percentages shown in Table 1 provide a rough estimate of the proportion of labeled cells in a given area, it is also important to take into consideration the density of labeling in a given region. For example, in case M-3-90 FB, which contained a retrograde tracer injection in area 36r (Fig. 9D, Table 1), the density of labeled cells in area TH was equivalent to that in area TF. However, because area TH is much smaller than area TF, the absolute number and, thus, the percentage of labeled cells in area TH was substantially lower than that of area TF (1% vs. 24%; Table 1). Thus, for the cases presented in this report, it is important to take into consideration both the data from the unfolded density maps as well as the percentages shown in Table 1 to gain a full understanding of the strength of retrograde labeling in a given region of the brain.

Entorhinal cortex

For all of the temporal lobe unfolded density maps, the subdivisions of the entorhinal cortex are shown for reference, although the density of labeling is not shown. We have previously summarized the organization of the reciprocal projections between the entorhinal cortex and the perirhinal and parahippocampal cortices (Suzuki and Amaral, 1994a). Similarly, the location of the parasubiculum (PAS) is shown on the unfolded maps but the labeling is not indicated.

Density maps of the frontal, insular, cingulate, and retrosplenial cortices

The metric for translation of cell densities to gray-level shading patterns used for the temporal lobe was also applied to the unfolded maps of the frontal, insular, cingulate, and retrosplenial cortices. Thus, in any particular case, the relative strength of projections originating from all of these cortical regions can be easily appreciated by comparison of the unfolded maps (see Figs. 9, 16).

RESULTS
Nomenclature

The entorhinal, perirhinal, and parahippocampal cortices surround the rhinal sulcus on the ventromedial surface of the macaque monkey brain (Fig. 1). The cytoarchitectonic organization and terminology for the various subdivisions of the entorhinal cortex have been described previously (Amaral et al., 1987). Because a detailed description of the cytoarchitectonic organization of the perirhinal and parahippocampal cortices will be presented at a later date, here, we briefly present the essential characteristics that were used to set their boundaries in the experimental preparations. Figure 3A shows an unfolded, two-dimensional map illustrating the boundaries and subdivisions of the macaque monkey entorhinal, perirhinal, and parahippocampal cortices.

Perirhinal cortex. The perirhinal cortex comprises a smaller, medially situated area 35 and a larger, laterally situated area 36 (Figs. 1A,B, 3A). For most of its rostrocaudal extent, area 35 is confined to the fundus and lateral bank of the rhinal sulcus; at the extreme rostral pole of the
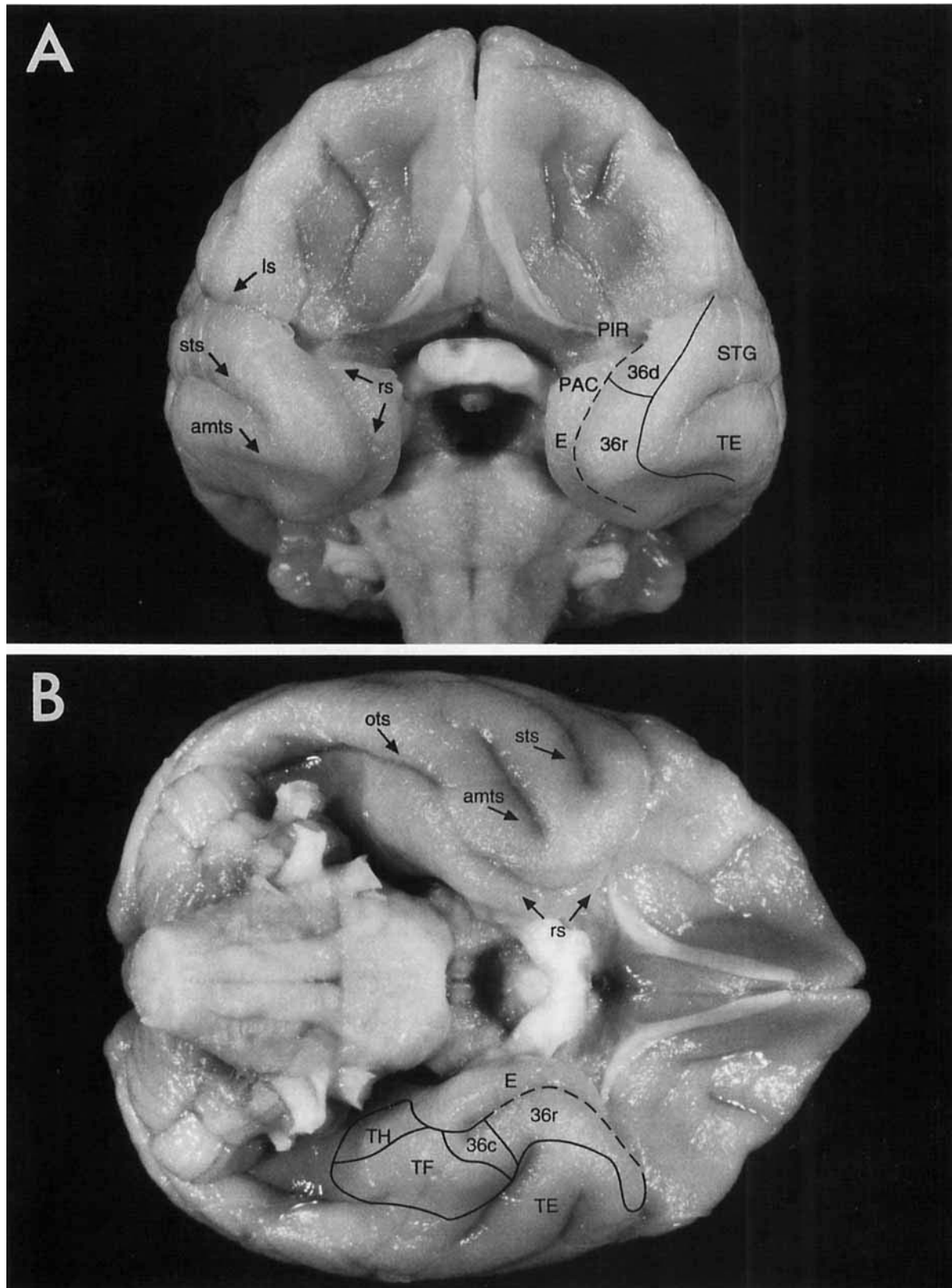
Fig. 1. **A:** Frontal view of the brain of the *Macaca fascicularis* monkey showing the location of areas 36d and the dorsal portion of area 36r of the perirhinal cortex. The perirhinal cortex is bounded medially by the rhinal sulcus (rs; dashed line) and is continuous laterally with the STG and area TE. **B:** Ventral view of the same brain on which is indicated the location of the entorhinal cortex (E), areas 36r and 36c of the perirhinal cortex, and areas TH and TF of the parahippocampal cortex. Area 35 of the perirhinal cortex is buried within the lateral bank of the rhinal sulcus and is not seen in this surface view. amts, anterior middle temporal sulcus; ls, lateral sulcus; ots, occipitotemporal sulcus; PAC, periamygdaloid cortex; PIR, piriform cortex; STG, superior temporal gyrus; sts, superior temporal sulcus; TE, area TE of Bonin and Bailey, 1947.

entorhinal cortex, area 35 extends slightly onto the medial bank of the rhinal sulcus. Area 35 is an agranular cortex that is characterized by a dense layer V populated by large, darkly staining cells. Layer V is generally separated from a poorly populated layer III by a cell-free zone; layer II is patchy and populated by small to medium-sized cells.

Area 36 is located just lateral to area 35 and has been parceled into five subdivisions (Fig. 3A). Area 36d (the dorsal subdivision of area 36) is located at the most rostral and dorsal extent of the perirhinal cortex (Fig. 1A) and makes up approximately the dorsal one-third of what is typically referred to as the temporal pole (area 38 of Brodmann, 1909; area TG of Bonin and Bailey, 1947). This area shares many of the same cytoarchitectonic characteristics with the other subdivisions of area 36, but its cell layers tend to be less organized and less laminated than the other subdivisions. Caudally, adjacent to area 36d, is area 36r (rostral subdivision of area 36). Area 36r has been further subdivided into 36rm (rostromedial subdivision of area 36) and area 36rl (rostrolateral subdivision of area 36). Area 36rm is situated lateral to area 35, is relatively narrow in the mediolateral axis, and is bordered laterally along its full rostrocaudal extent by area 36rl. This area is characterized by prominent clumps of darkly staining, small cells in layer II, large, lightly staining, roundish cells in layer III, and large, darkly staining, fusiform-shaped cells in the deep layers. Area 36rl is the largest of the subdivisions of area 36. At its most rostral and dorsal extent, it makes up approximately the ventral two-thirds of what is typically referred to as the temporal pole (most of what is labeled 36r in Fig. 1A, area 38 of Brodmann, 1909; area TG of Bonin and Bailey, 1947). It is bounded laterally by the unimodal visual area TE. Ventrally, area 36rl is situated at the same level as approximately the rostral one-half of the entorhinal cortex (Figs. 1B, 3A). Area 36rl can be distinguished from area 36rm by a more prominently bilaminate appearance of layer III, a thicker layer IV, and layers V and VI with characteristically multipolar rather than fusiform cells. Area 36rl can be distinguished from the laterally adjacent area TE, because the latter has a clear separation between layers V and VI. Layer II in TE is thicker than in area 36rl, is made up of smaller cells, and lacks the patches of darkly stained cells observed in area 36rl. Area TE also has a more columnar organization.

The caudal extreme of the perirhinal cortex is called area 36c (caudal subdivision of area 36; Fig. 1B). As with area 36r, we have identified medial and lateral portions of area 36c: area 36cm (caudomedial subdivision of area 36) and area 36cl (caudolateral subdivision of area 36; Fig. 3A). Area 36cm is laterally adjacent to the intermediate and caudal divisions of the entorhinal cortex (areas E_I and E_C), and area 36cl is typically bounded laterally by the rostral pole of area TF. In general, areas 36cm and 36cl are the most highly laminated subdivisions of the perirhinal cortex. Layer IV tends to be thicker in these subdivisions, and the cortex has a more prominent radial organization. For clarity, we have only indicated the boundaries of areas 35, 36d, 36r, and 36c in the unfolded temporal lobe maps of Figures 2, 5, 9D, 11, 12, and 16D.

It should be noted that the area encompassed by the perirhinal cortex, as defined here, is substantially larger than illustrated in previous papers on this region (Jones and Powell, 1970; Van Hoesen and Pandya, 1975; Murray and Mishkin, 1986; Riches et al., 1991; Gaffan and Murray, 1992; Meunier et al., 1993). This is due largely to the fact that we have placed the border of the perirhinal cortex with area TE substantially more lateral than is typically the case. The judgement to place the border at this position is based on the finding that the entire region that we have defined as the perirhinal cortex has similar connections both with the entorhinal cortex and with the neocortex. These connections seem to be substantially different from those of the laterally adjacent area TE. Historically, much of what we have labeled perirhinal cortex has been included under the rubric of "inferotemporal cortex" (IT cortex or area TE). The inferotemporal cortex is generally agreed to constitute higher-order unimodal visual association cortex. Given that the entire region that we have labeled perirhinal cortex receives inputs from both unimodal and polymodal cortical regions, it would appear inappropriate to include it as a portion of IT cortex.

Parahippocampal cortex. The parahippocampal cortex is caudally adjacent to both the entorhinal cortex and the perirhinal cortex and is made up of a smaller, medially situated area TH and a larger, laterally situated area TF (Fig. 1B). Area TH has been divided into a rostral subdivision (area THr) and a caudal subdivision (area THc; Fig. 3A). Area THr is an agranular cortex made up of essentially two layers. The superficial layers II/III are comprised of a thin outer portion made up of small cells and a more homogeneous inner portion made up of a dense population of round cells that tend to blend together with the smaller cells of the outer portion. The deep layers V/VI of area THr are made up of a dense band of large, darkly stained cells; these cells are the largest cells found in the parahippocampal cortex. Area THc is situated just caudal to area THr and can be distinguished from area THr by the presence of an internal granule-cell layer (layer IV), more radially oriented cells, and an overall more highly laminated appearance. Like area THr, area THc has rather homogeneous-looking deep layers, but the cells of the deep layers of area THc are smaller and less densely packed than the cells of area THr.

We have subdivided area TF into areas TFm (medial subdivision of area TF) and TFl (lateral subdivision of area TF; Fig. 3A). In general, area TF is a dysgranular cortex that is distinguished by large, darkly staining cells in layers V and VI. Area TFm can be distinguished from area TFl, because it is thinner, the cells of layer III do not show a distinctive size gradient, layer IV is less prominent, and there is less differentiation between layers V and VI. Area TFl can be distinguished from the laterally adjacent areas TE or TEO, because the deep cells of area TE are smaller, the cortex is more radially organized, and layer IV becomes more prominent in area TE. Caudally, area TF is bounded by area OA (Bonin and Bailey, 1947), also referred to as area V4 (Zeki, 1971). For clarity, we have only indicated the boundaries for the subdivisions of areas TH and TF on the temporal lobe unfolded maps in Figures 2, 5, 9D, 11, 12, and 16D.

Areas TE and TEO. Unimodal visual areas TE and caudally adjacent area TEO form a wide band of cortex bordered medially by the perirhinal and parahippocampal cortices and bordered laterally by the fundus of the superior temporal sulcus. Several authors have subdivided area TE based on cytoarchitectonic, connectional, or behavioral criteria (Seltzer and Pandya, 1978; Felleman et al., 1986; Iwai, 1981; Horel et al., 1987; Iwai and Yukie, 1987; Yukie et al., 1988; Desimone and Ungerleider, 1989; Yukie et al., 1990; Felleman and Van Essen, 1991; Van Essen et al., 1991; Weller and Steele, 1992). However, we have found

differentiating these subdivisions solely on cytoarchitectonic criteria to be very difficult. Consistent with previous reports (Weller and Steele, 1992, and references therein), we have observed mediolateral (dorsoventral) differences in the topography of projection patterns within areas TE and TEO that prompted us to subdivide these areas. We have maintained the terms TE and TEO for the larger subdivision spanning the ventromedial region bounded medially by the perirhinal and parahippocampal cortices and bounded laterally by the ventral lip of the superior temporal sulcus (Fig. 2D). This region has previously been subdivided into areas TE1, TE2, and TE3 (Seltzer and Pandya, 1978). It should be noted that approximately the medial half of area TE1 of Seltzer and Pandya (1978) corresponds to approximately the lateral half of what we have labeled as area 36 of the perirhinal cortex. The other subdivision consisted of the cortex lining the ventral bank of the superior temporal sulcus, which we refer to as STSv (Fig. 2D). Seltzer and Pandya (1978) have previously designated this region areas TEa and TEm.

Superior temporal sulcus (STS). Although a variety of different studies have attempted to subdivide the cortex of the superior temporal sulcus based on cytoarchitectonic criteria (Pandya and Sanides, 1973; Jones and Burton, 1976; Seltzer and Pandya, 1978), these studies were all originally carried out in the rhesus monkey, and it has proven difficult to apply these same criteria to the *Macaca fascicularis* monkey (Insausti et al., 1987). However, results from both connectional and electrophysiological studies have consistently shown that the dorsal bank and fundus of the superior temporal sulcus (labeled STSd and STSf in Fig. 2D) are polymodal associational areas (Seltzer and Pandya, 1978; Bruce et al., 1981; Baylis et al., 1987). This region has also been referred to as the superior temporal polysensory area, or STP, of Bruce et al. (1981) and corresponds roughly to areas IPa, PGa, TPO, and TAa of Seltzer and Pandya (1978). On our unfolded maps, we have labeled the dorsal bank and fundus of the superior temporal sulcus STSd and STSf, respectively (Fig. 2D).

Superior temporal gyrus. Both neuroanatomical studies (Pandya et al., 1969; Pandya and Sanides, 1973) and electrophysiological studies (Merzenich and Brugge, 1973) have shown that much of the cortex of the caudal portion of the STG is auditory association cortex. Rostral portions of STG however, appear to have cells that respond to both auditory and visual stimuli (Baylis et al., 1987). There are also differences in the connectivity of the rostral STG vs. the caudal STG. Whereas approximately the rostral half of the STG has direct connections with the entorhinal cortex, more caudal regions do not (Insausti et al., 1987). Thus, although we appreciate differences in the responsiveness and connectivity of the rostral and caudal STG, because of the difficulty in distinguishing these subdivisions on cytoarchitectonic grounds, we have labeled the entire region STG on the unfolded maps (Fig. 2D).

Frontal lobe. Figure 6, top, shows a representative unfolded map of the frontal lobe. We have used the cytoarchitectonic descriptions and nomenclature of Walker (1940) with slight modifications (Carmichael, 1993).

Insular cortex. Figure 7, top, shows a representative unfolded map of the insular cortex. We have followed the cytoarchitectonic descriptions and nomenclature of Jones and Burton (1976) for these areas.

Cingulate and retrosplenial cortices. Figure 8, top, shows a representative unfolded map of the cingulate

cortex. The nomenclature for these regions has been derived from the works of Pandya et al. (1981) and Vogt (1985) as adapted by Insausti et al. (1987).

Posterior parietal cortex. Figure 15 shows the distribution of retrogradely labeled cells in a series of coronal sections through the parietal lobe after an injection in area TF of the parahippocampal cortex. The divisions of the posterior parietal lobe have been derived from Brodmann's original description (1909) as recently elaborated by Andersen et al. (1990).

Description of injection sites

Figure 3B presents an unfolded map of the entorhinal, perirhinal, and parahippocampal cortices to illustrate the sizes and locations of the 31 retrograde tracer injections that were analyzed in this study. Before describing the distribution of retrogradely labeled cells resulting from these injections, we briefly describe the size and laminar location of the subset of 17 injections for which unfolded density maps are presented. These experiments were selected to provide an overview of the inputs to the perirhinal and parahippocampal cortices. The remaining 14 experiments provided largely confirmatory information on the distribution of retrogradely labeled cells. For all cases, we describe only the position of the core of the dye injections, which has been referred to as zone 1 of the injection site (Huisman et al., 1983). It has been claimed, and our experience has confirmed, that effective transport for both fast blue and diamidino yellow injection sites arises mainly from zone 1 (Huisman et al., 1983).

Injections in area 36d. We analyzed two injections (cases M-21-91 DY and M-22-91 FB; Fig. 3B) confined primarily to area 36d just dorsal to the dorsal border of area 36rm. The injection in case M-21-91 DY involved all layers of cortex for approximately 2 mm in the rostrocaudal direction; there was minor leakage into underlying white matter. The injection in case M-22-91 FB was confined to area 36d and located slightly lateral to the injection in case M-21-91 DY.

Injections in area 36r. There were four injections located in the most rostral and dorsal portions of area 36rm (cases M-20-91 DY, M-20-91 FB, M-21-91 FB, and M-22-91 DY; Fig. 3B). The injection in case M-21-91 FB involved all layers of area 36rm cortex for approximately 2.5 mm in the rostrocaudal direction; the white matter underlying area 35 was also partially involved in this injection site. There were six retrograde tracer injections placed throughout the ventral portion of area 36r; five of these were situated in area 36rm, and one was in area 36rl. Two of the injections in area 36rm (M-4-90 DY and M-5-90 DY; Fig. 3B) also involved the lateral aspect of area 35. Case M-3-90 DY was a small injection, approximately 300 μm in diameter, centered in layer V of area 36rm. There was no leakage of tracer into the white matter in this case. Case M-3-90 FB (Fig. 3B) was a larger injection, approximately 1 mm in diameter, that involved all layers of cortex and was centered in area 36rl. This injection had little or no involvement of the white matter or of adjacent brain structures. Case M-4-91 DY contained an injection of DY, approximately 300 μm in diameter, focused primarily in layers I–III in the most medial aspect of area 36rm.

Injections of area 36c. There were three injections in area 36c (M-12-90 DY, M-8-91 DY, and M-7-91 DY; Fig. 3B); one of these injections involved area 36cm, and the others were situated in area 36cl. The injection in case M-12-90 DY
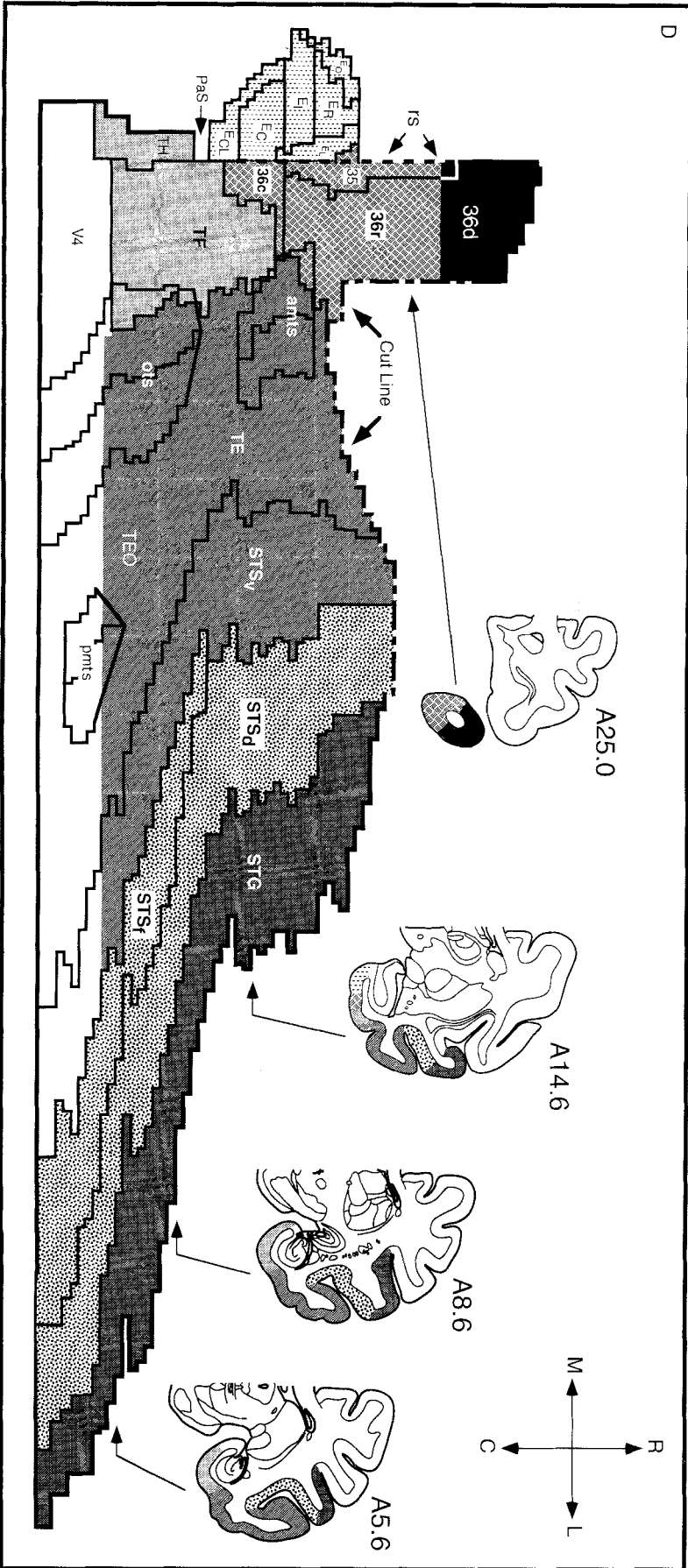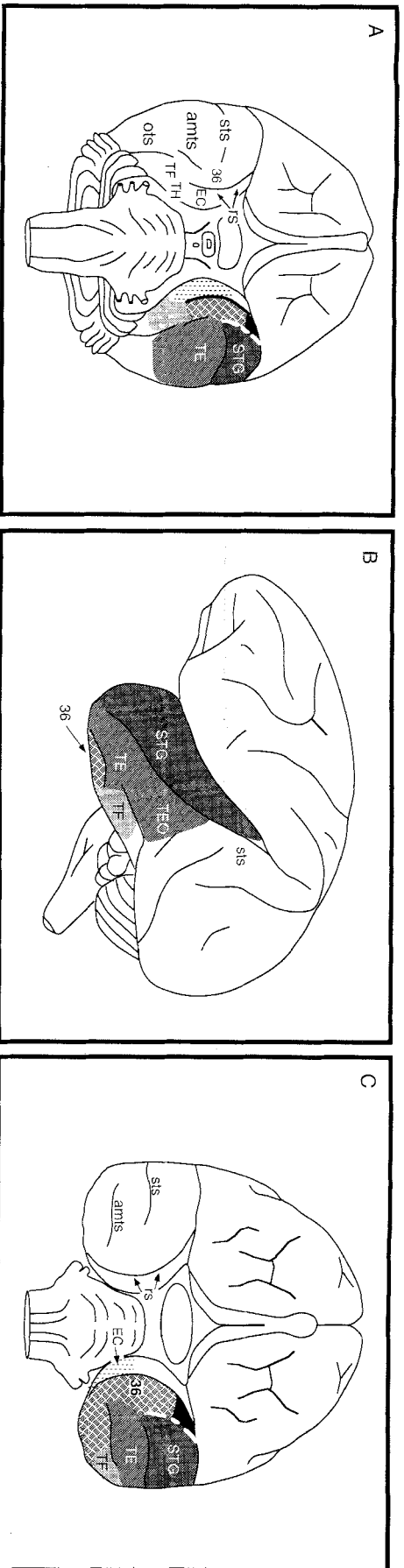
Figure 2

was located in the rostral and medial aspect of area 36cm and involved primarily layers II and III of the cortex. There was little or no contamination of the deeper layers of the cortex. Case M-8-91 DY contained a medium-sized injection (approximately 1 mm in diameter) that involved layers I–III of the cortex at the lateral aspect of area 36cl. This was also a very discrete injection with no involvement of the white matter.

Injections of area 35. Because area 35 is a relatively narrow region buried in the fundus of the rhinal sulcus, it was difficult to discretely deliver retrograde tracer to this cortical area. There were two injections, however, that primarily involved area 35 (cases M-1-90 DY and M-4-91 FB; Fig. 3B) and two cases that involved area 35 and adjacent portions of area 36rm (cases M-4-90 DY and M-5-90 DY; Fig. 3B). Case M-4-91 FB was located caudally in area 35 and involved all layers of the cortex. There was also some minor involvement of the most lateral aspect of the entorhinal cortex. The injection in case M-5-90 DY was also located caudally in area 35 and involved both the lateral aspect of area 35 and the most medial aspect of area 36rm. This injection was approximately 800 μm in diameter and involved primarily layers III–V. There was no involvement of the white matter or adjacent structures in this case.

Injections of area TF. There were a total of 11 retrograde tracer injections in and around area TF (Fig. 3B); five of these were situated in area TFl, and four were in area TFm. Case M-12-90 FB contained an injection approximately 800 μm in diameter that involved layers I–IV and the superficial portion of layer V at the border of area 36c with area TF. Although, based on cytoarchitectonic criteria, this injection appeared to straddle the border between areas 36c and TF, the overall labeling resulting from this injection more closely resembled the connectivity of area TF than area 36. Case M-10-90 DY had a DY injection approximately 500 μm in diameter that was located in the rostromedial portion of area TF. The injection involved primarily layer VI and included some underlying white matter. The

injection in case M-10-90 FB was located laterally and caudally to the DY injection. The fast blue injection was approximately 1 mm in diameter and located primarily in layers V and VI of cortex. This injection also involved some of the underlying white matter. Case M-2-90 DY contained a DY injection approximately 700 μm in diameter that was slightly more laterally situated in area TF. This injection involved layers V and VI but had little or no involvement of the underlying white matter. Case M-2-90 FB contained an injection situated more caudally in area TF. This injection was slightly larger than the DY injection (approximately 1 mm in diameter) and involved layers III–VI. There was also some minor involvement of the underlying white matter. Case M-1-92 FB contained a FB injection at, or just lateral to, the lateral border of area TF at a midrostrocaudal level. This injection was approximately 850 μm in diameter and involved layers III–VI of cortex. There was little or no involvement of the white matter. Case M-1-92 DY contained an injection located caudal to the injection in case M-1-92 FB. This injection was also situated at, or just lateral to, the lateral border of area TF, was smaller than the fast blue injection (approximately 700 μm in diameter), and involved primarily layers III and IV. There was no involvement of the overlying white matter or adjacent structures in this case.

Injections of area TH. There were three retrograde tracer injections located within area TH (Fig. 3B). Case M-3-91 FB had an injection that was located caudally and laterally in area TH. This injection was approximately 1 mm in diameter and involved layers III-IV of the cortex.

Because some of these injection sites only involved the deep layers of cortex, the question may arise whether the more superficially placed terminals of the corticocortical connections had access to the dyes. However, it is well known that fibers passing through the core of a fluorescent dye injection site will robustly support retrograde transport (Kuypers, 1984), and, thus, both deep and superficial injections should demonstrate much of the full complement of cortical inputs to the injected regions.

Overview of the presentation of results

We will now describe the organization of cortical afferents to the macaque monkey perirhinal and parahippocampal cortices. Because there were substantial differences in the origins of cortical projections to the perirhinal and parahippocampal cortices, we first describe the organization of cortical inputs from the temporal, frontal, insular, cingulate, retrosplenial, and parietal cortices to areas 35 and 36. We then describe the origin of projections from these same cortical regions to areas TF and TH.

Organization of cortical afferents to the macaque monkey perirhinal cortex

Temporal lobe afferents to the perirhinal cortex. Figure 5 shows a series of two-dimensional, unfolded density maps of the temporal lobe illustrating the distribution and relative density of retrogradely labeled cells resulting from six injections placed at different locations throughout the perirhinal cortex. The pattern of retrograde labeling in the temporal lobe following injections in areas 35, 36r, and 36c was generally similar. Thus, we will first summarize the general pattern of temporal lobe labeling resulting from injections in these areas. The pattern of temporal lobe labeling following injections of area 36d exhibited certain unique characteristics and will be considered separately.

Fig. 2. **A–C:** Line drawings of a ventral, lateral, and frontal view, respectively, of the *Macaca fascicularis* brain. The shading patterns in these surface views correspond to the shading patterns shown in the two-dimensional, unfolded map of the temporal lobe in D. **D:** Representative, straight-line, unfolded map of the temporal lobe of the *Macaca fascicularis* brain. Subdivisions of the entorhinal cortex (areas E_O, E_R, E_L, E_I, E_C, E_{CL}), perirhinal cortex (areas 35, 36d, 36r, and 36c), and parahippocampal cortex (areas TH and TF) are indicated. Solid lines represent either the boundaries of cortical areas or the boundaries of sulci. The fundus of the rhinal sulcus (rs) is represented by a dashed line. The dashed-dotted-dashed line at the top of the map (cut line) represents a region where the cortical map has been "cut" to better represent the polar portion of the temporal lobe. This line corresponds to the white dashed-dotted-dashed line shown in A and C. Shown on the right are a series of line drawings of representative coronal sections adapted from the atlas of Szabo and Cowan (1984). Arrows indicate the approximate level of the unfolded map at which the section would be located. Shading patterns in each coronal section correspond to regions of the unfolded map with the same shading patterns. The designations A25.0, A14.6, etc., indicate distances in millimeters anterior (A) to the interaural line. In this and all subsequent figures, the compass indicates the axes of the unfolded maps. PaS, parasubiculum; pmts, posterior middle temporal sulcus; STSf, fundus of the superior temporal sulcus; STSd, dorsal bank of the superior temporal sulcus; STSv, ventral bank of the superior temporal sulcus; TE, area TE of Bonin and Bailey, 1947; TEO, area TEO of Bonin and Bailey, 1947; V4, area V4 of Zeki, 1971; R, C, M, and L refer to rostral, caudal, medial, and lateral, respectively.
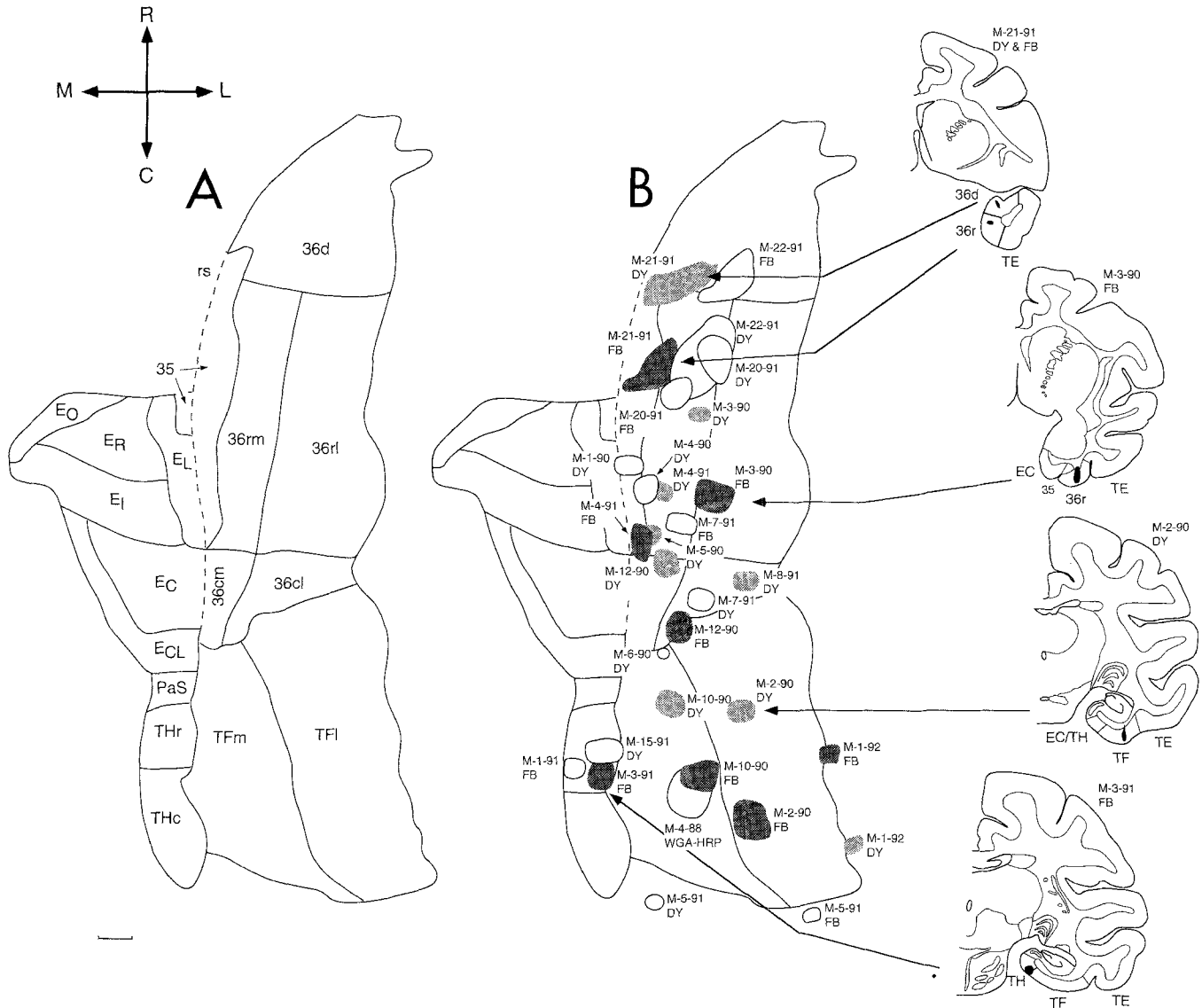
Fig. 3. **A:** Representative unfolded map of the entorhinal cortex, perirhinal cortex (areas 35, 36d, 36rm, 36rl, 36cm, and 36cl), and parahippocampal cortex (areas THr, THc, TFm, and TFl). See text for descriptions of the subdivisions of the perirhinal and parahippocampal cortices. The dashed line represents the fundus of the rhinal sulcus (rs). **B:** Unfolded map showing the location of the 31 injection sites used for this study. Shaded injection sites designate the subset of 17 cases for which two-dimensional, unfolded density maps are presented in the following figures. The darker shading pattern represents fast blue (FB)

injections, and the lighter shading pattern represents injections of diamidino yellow (DY). Cases M-1-92 FB and M-1-92 DY are located on the border of area TF with areas TE and TEO, respectively. Cases M-5-91 FB and M-5-91 DY are located in area V4 just caudal to area TF. Shown on the right are line drawings of coronal sections located at four rostrocaudal levels of the temporal lobe. They show injection sites (solid profiles) from four of the analyzed cases. Scale bar = 1.2 mm (applies only to the unfolded maps).

Labeling in areas TE and TEO. Even a casual glance at the unfolded density maps in Figure 5 reveals that area TE and rostral portions of area TEO provide prominent projections to the perirhinal cortex. Moreover, there appeared to be two subregions of inferotemporal unimodal visual cortex that consistently projected to the perirhinal cortex. One of these regions was located medially in areas TE and rostral TEO, and the other was situated in the cortex lining the ventral bank of the superior temporal sulcus (STSv). We first consider the organization of the projection from areas TE and TEO to the perirhinal cortex.

The distribution of retrogradely labeled cells in area TE exhibited a prominent mediolateral topography and a more subtle rostrocaudal topography. Injections in areas 35 (Fig. 5D), 36r (Fig. 5B,C), and 36c (Fig. 5E,F) consistently resulted in a dense, longitudinally oriented band of labeled cells located in medial portions of areas TE and rostromedial portions of area TEO. The more laterally situated portions of areas TE and TEO, nearer the ventral lip of the superior temporal sulcus, either contained lower densities of labeled cells than the medial portions (Fig. 5B–D) or, in some cases, few if any labeled cells (Fig. 5E,F). The heavily
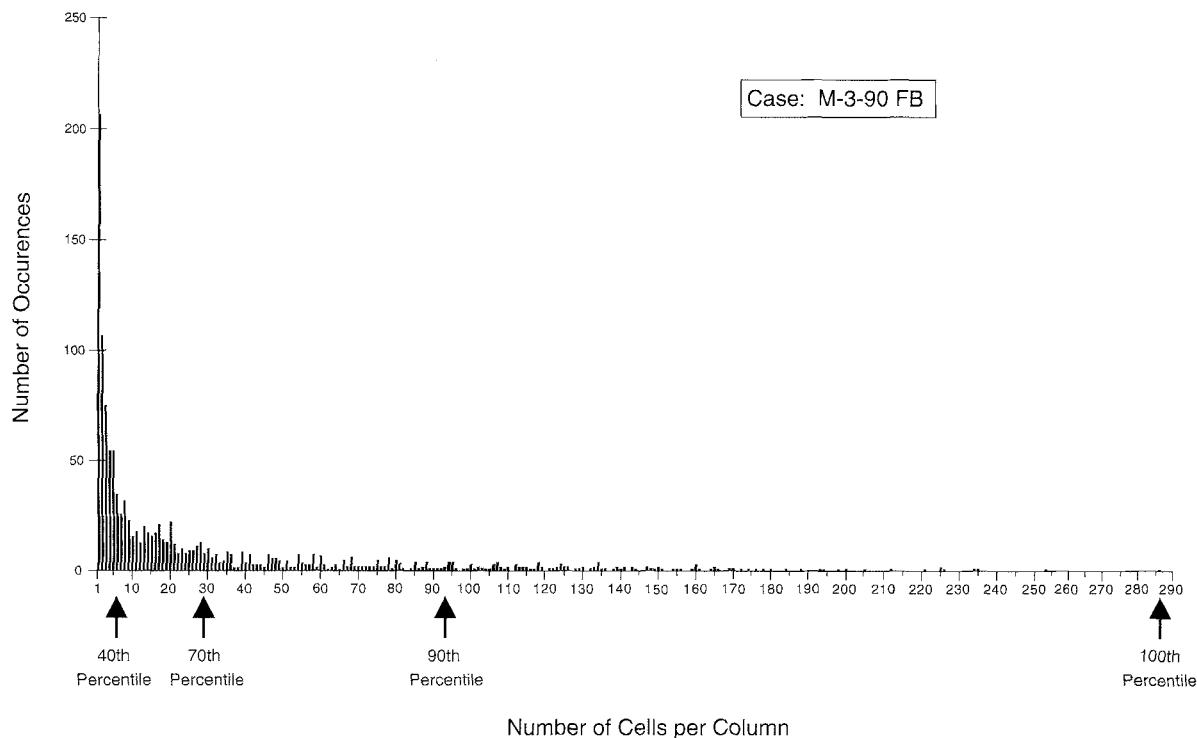
Fig. 4. Histogram showing the number of occurrences (Y-axis) of counts of retrogradely labeled cells per 769-μm-wide column of cortex (X-axis) throughout the temporal lobe in case M-3-90 FB. The arrows indicate the number of labeled cells per column of cortex corresponding to the 40th, 70th, 90th, and 100th percentiles in this case (see text for details).

labeled portion of area TE corresponded roughly to areas TE1 and TE2 of Seltzer and Pandya (1978). These data suggest that the perirhinal cortex receives a substantial convergence of information from a band of cortex along the medial portion of areas TE and rostral TEO. Conversely, the medial portion of areas TE and rostral TEO project in a highly divergent fashion to all regions of areas 35, 36r, and 36c.

The rostrocaudal topography of the projection from areas TE and TEO can be appreciated by comparing the distribution of retrogradely labeled cells in Figure 5B,C,F. These experiments had retrograde tracer injections at three different rostrocaudal levels through areas 36r and 36c. The most rostrally situated injection (Fig. 5B) resulted in the highest density of retrograde labeling rostrally in area TE, whereas injections situated at progressively more caudal levels of the perirhinal cortex (Fig. 5C,F) produced the highest density of labeling more caudally in areas TE and TEO.

Labeling in area STSv. A second focus of retrogradely labeled cells was situated in the unimodal visual areas on the ventral bank of the superior temporal sulcus (STSv). Interestingly, unlike the longitudinally organized projection from medial portions of area TE, the labeling within the ventral bank of the STS, particularly after injections in areas 35 and 36r, tended to occur in "patches." This patchy organization can be appreciated in the temporal lobe unfolded map illustrated in Figure 5C, which contained an injection in area 36r (See also Figs. 9, 10). In this case, there was a moderate to high density of retrogradely labeled cells in a "patch" of cortex in the most rostral portion of STSv at

the level of area E_R and a second, less densely populated patch of labeled cells located more caudally at the level of areas E_C and E_CL of the entorhinal cortex. The location of these two labeled patches within the STSv appeared to be fairly consistent in other cases with injections of areas 36r (Fig. 5B) or cases with injections in area 35 (Fig. 5D). The labeling in area STSv following injections in area 36c, in contrast, was less dense and was not organized in patches (Fig. 5E,F). This pattern suggests that there are two patches of cortex in the STSv that project divergently to large portions of areas 35 and 36r.

Labeling in the parahippocampal cortex. Another prominent input to the perirhinal cortex arose from areas TF and TH. In all cases, the rostral portions of area TF and TH demonstrated a high density of retrogradely labeled cells, whereas more caudal regions contained moderate to low densities of labeled cells (Figs. 5B–F). This general pattern of labeling was consistent for cases with injections in areas 35 (Fig. 5D), 36r (Fig. 5B,C), and 36c (Fig. 5E,F). It should be noted that, although areas TF and TH contained equally high densities of retrogradely labeled cells, because TH is a much smaller area than TF, the total number of retrogradely labeled cells observed in area TH represents a much smaller percentage of total labeled cells compared to the percentage of labeled cells observed in area TF (Table 1).

Labeling in the fundus and dorsal bank of the superior temporal sulcus (STSf and STSd). The relative density of labeling in the fundus and dorsal bank of the STS appeared to differentiate the injections in areas 36r and 36c from those in area 35. In all cases with injections in area 36r (Fig. 5B,C) or 36c (Fig. 5E,F), a moderate to low density of
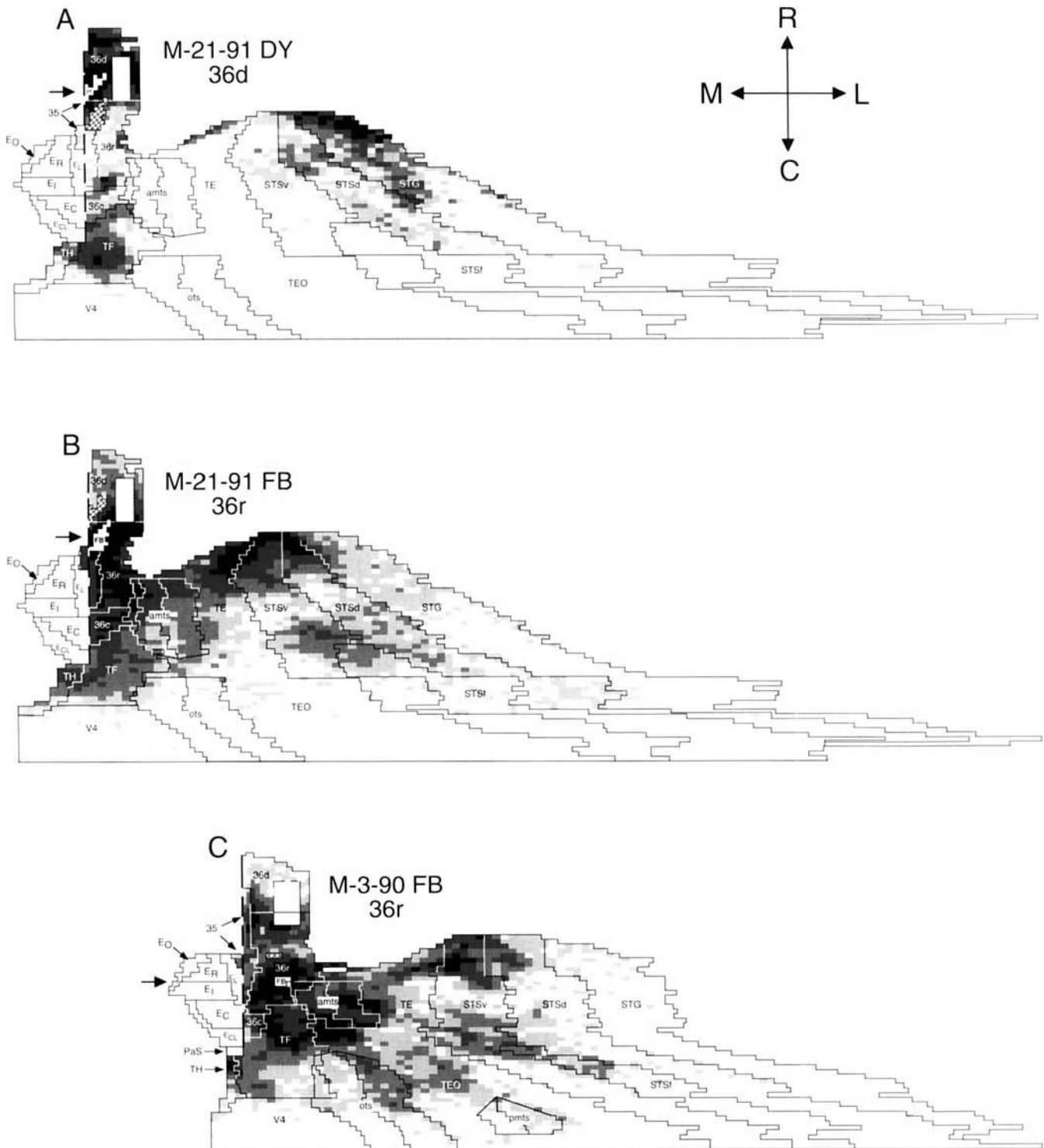
Fig. 5. **A–F:** A series of two-dimensional, unfolded density maps of the temporal lobe representing labeling resulting from six injections in the perirhinal cortex. The cases are arranged from injections placed rostrally (A) to caudally (F) in the perirhinal cortex. The case name and injection site are indicated adjacent to each map. The locations of the injection sites on the map are shown in white and are marked with either "FB" to indicate a fast blue injection, or "DY" to indicate a diamidino yellow injection. As an aid to locating the injection site, its rostrocaudal position is indicated by a large black arrow to the left of the map. The cross-hatched area represents the location of the other injection site in that case that precluded analysis of retrogradely labeled cells in that region. The white rectangular area in the temporal pole of each map represents a region of cortex (i.e., the tip of the temporal pole) that could not be unfolded, because coronal sections through this region are cut obliquely, and layer IV is not visible. Black voxels represent regions of cortex containing the highest density of retrogradely labeled cells, whereas progressively lighter shades of gray represent progressively lower densities of labeled cells (see text for details). The hatched region in area TF of case M-12-90 DY represents a region of cortex that was damaged and could not be analyzed. All abbreviations and conventions are the same as in Figure 2. Scale bar = 2 mm.
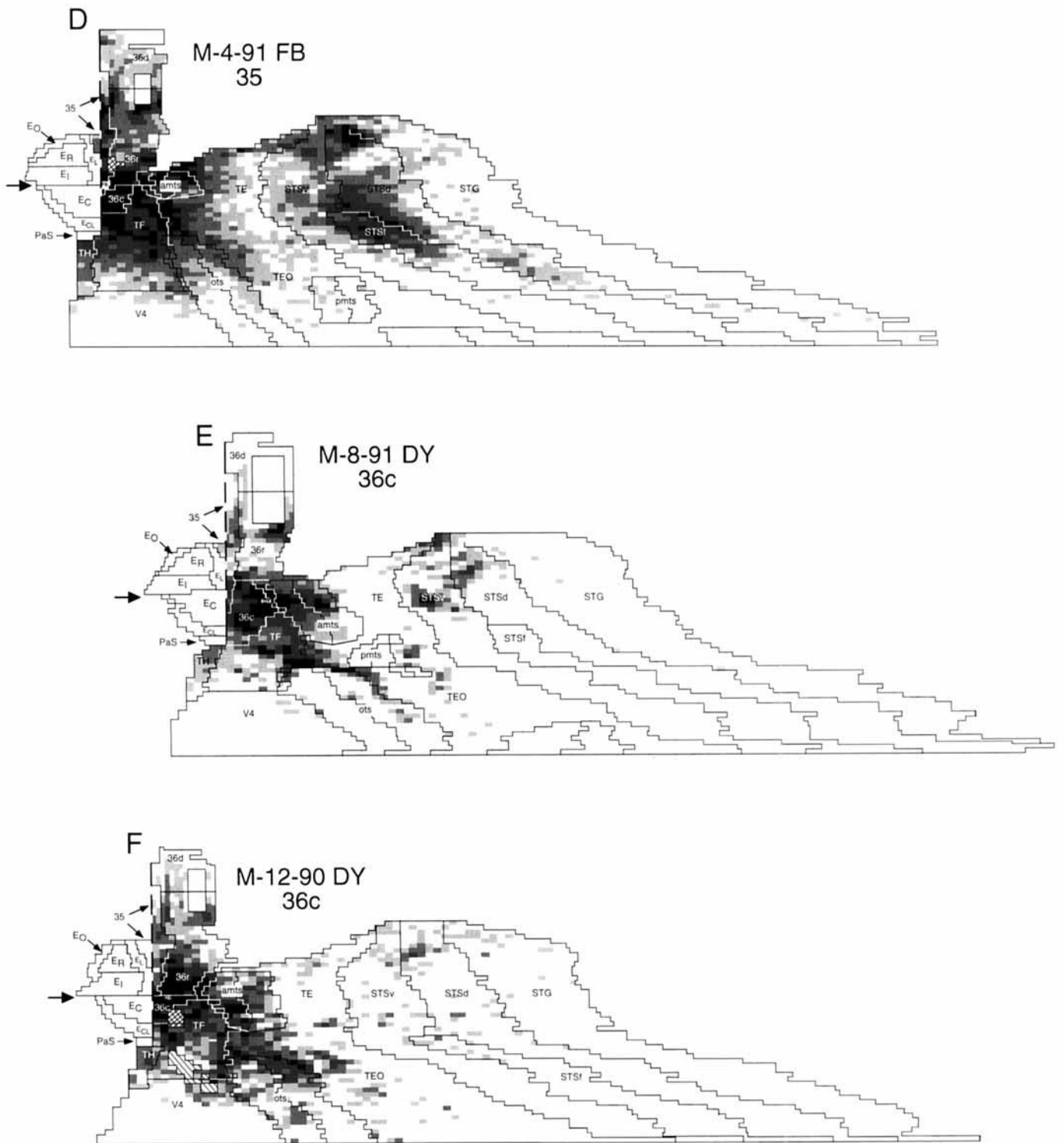
Figure 5. continued

labeled cells was consistently observed in STSd. The topographical organization of this projection to area 36r appeared to roughly parallel the patchy topography of projections from the ventral bank of the STS i.e., two patches of labeling were observed in STSd that tended to occur at the same rostrocaudal level as the patches on the ventral bank of the STS (Fig. 5B,C). The density of labeling on the dorsal bank of the STS after injection in areas 36r and 36c, however, was typically either similar (Fig. 5E,F) or lower (Fig. 5B,C) than the labeling seen on the ventral bank. After injections primarily involving area 35, however (Fig. 5D), the density of labeling on the dorsal bank and fundus of the STS was higher than in the cases with injections confined to area 36 (compare Fig. 5C with Fig. 5D). Moreover, the density of labeled cells in STSd and STSf was higher than the density of labeled cells observed in STSv (Fig. 5D). The relatively stronger projection from the fundus and dorsal bank of the STS to area 35 than to area 36 was the only notable difference in the organization of temporal lobe afferents to these areas.

The higher proportion of labeling in polymodal areas after injections in area 35 may reflect the fact that, cytoarchitectonically, area 35 is a transitional zone between area 36, on the one hand, and the entorhinal cortex, on the other. Area 36 receives strong input from area TE, whereas the entorhinal cortex receives essentially no direct input from area TE and a strong projection from polymodal areas like the fundus and dorsal bank of the superior temporal sulcus.

Labeling in the superior temporal gyrus. Injections into areas 35, 36r, and 36c of the perirhinal cortex resulted in relatively few labeled cells in the STG, and in all cases, they were observed at the most rostral levels (Fig. 5B–F).

Labeling after injections in area 36d. As noted previously, the retrograde tracer injections into area 36d resulted in a distinct distribution of labeled cells. In case M-21-91 DY (Fig. 5A), for example, in contrast to the strong visual inputs to the rest of the subdivisions of the perirhinal cortex, there was only a moderate to low density of retrogradely labeled cells in unimodal visual areas. The highest densities of retrogradely labeled cells were observed in the most rostral portion of the STG, in area TF and TH, and in the dorsal bank of the STS (Fig. 5A). Although the pattern of temporal lobe labeling in case M-21-91 DY appeared to be quite different from the pattern of labeling observed after an injection in the most rostral/dorsal portion of area 36r (Fig. 5B), there does appear to be a relatively gradual shift in the pattern of labeling from area 36r to area 36d. An additional case that contained an injection located just dorsal to the injection illustrated in Figure 5B (Case M-20-91 DY) demonstrated a high density of labeled cells in the STG (as with the area 36d injection) but also demonstrated substantial labeled cells in area TE (as in the area 36r injection). Thus, it appears that area 36d receives much weaker unimodal visual inputs than the rest of the subdivisions of the perirhinal cortex and relatively stronger inputs from polymodal regions such as areas TF and TH and the rostral portions of the STG. It is these types of connectional differences that prompted the designation of this region as a separate subdivision of the perirhinal cortex. Clearly, however, further work is needed in this area to determine whether it is more appropriate to consider area 36d to be related to the rest of the perirhinal cortex (as we do here), or possibly to be related to the STG (with which it is also continuous), or even as an autonomous cortical region.

Laminar organization of retrogradely labeled cells in the temporal lobe. In general, retrogradely labeled cells throughout the temporal lobe were observed in layers III, V, VI, and, to a lesser extent, layer II (Fig. 10). There was a tendency for higher numbers of labeled cells to be observed in the deep layers, particularly in area TE (see Fig. 10b–d).

Summary of temporal lobe afferents to the perirhinal cortex

Injections involving all subdivisions of areas 35 and 36, except for area 36d, produced a similar pattern of retrogradely labeled cells in the temporal lobe. To obtain a more quantitative appreciation of the magnitude of projections from different portions of the temporal lobe, we have calculated the percentages of retrogradely labeled cells in different cortical areas for a representative case with an injection in area 36r (Case M-3-90 FB; Table 1, Figs. 5C, 9D). The strongest temporal lobe input to the perirhinal cortex originates in unimodal visual areas TE and TEO (62%; this percentage includes cells labeled in STSv). Areas TF and TH also contained high densities of retrogradely labeled cells representing 24% and 1%, respectively, of the total number of labeled cells throughout the brain. Moderate numbers of labeled cells were observed in the polymodal areas of the dorsal bank of the superior temporal sulcus (6%), and small numbers of cells were observed in the rostral portions of the STG (< 1%). A striking finding was that injections situated at any position in areas 35, 36r, or 36c produced a dense band of labeling in the medial portion of areas TE and rostral TEO. This pattern of labeling suggests that there is a substantial convergence of information from the medial aspect of areas TE and rostral TEO onto areas 35, 36r, and 36c. Area 35 tends to receive relatively stronger input from polymodal areas in the fundus and ventral bank of the STS than does area 36. Area 36d, located at the dorsal extreme of the perirhinal cortex, exhibits certain unique connectional attributes. Most notably, it receives only modest inputs from unimodal visual areas and strong inputs from the most anterior portions of the STG. Similar to the rest of the perirhinal cortex, however, area 36d receives strong inputs from areas TF and TH.

Frontal lobe afferents to the perirhinal cortex. Figure 6, bottom, presents a series of unfolded, straight-line density maps of the frontal lobe that illustrates the distribution of labeled cells in four representative injections located at different positions throughout areas 35 and 36 of the perirhinal cortex. In each case, the cell-count data in the frontal lobe were converted to gray-scale values using the same metric applied to the temporal lobe unfolded density maps.

Our general finding was that, regardless of where the retrograde tracer was placed in the perirhinal cortex, the pattern of labeled cells in the frontal lobe was similar (Fig. 6, bottom). In all cases, moderate densities of labeled cells were observed in caudal portions of area 13. Lower densities of labeled cells were also consistently observed in areas 11 and 12 of the inferior convexity. Some retrogradely labeled cells were also observed in area 45. After an injection in area 36d (Fig. 6A), however, no labeled cells were observed in area 45. Only occasionally were labeled cells observed in area 14, area 46 of the principal sulcus or areas 9, 6, and 8 on the dorsal surface of the frontal lobe.

Figure 10a shows a representative coronal section through the frontal lobe in case M-3-90 FB illustrating the laminar distribution of labeled cells. In general, labeled cells were

observed in both deep layers V and VI and superficial layer III. However, the labeling was consistently stronger in the deep layers.

Insular cortex afferents to the perirhinal cortex. Figure 7, bottom, shows a representative series of unfolded density maps of the insular cortex illustrating cases with injections located at different positions throughout the perirhinal cortex. A similar pattern of retrograde labeling in the insular cortex was observed after retrograde tracer injections in areas 35, 36r, and 36c. Figure 7B illustrates a typical pattern of labeling in the insular cortex. Moderate to small numbers of retrogradely labeled cells were consistently observed throughout areas Ia, Id, and Ig. Fewer labeled cells were observed in the parainsular cortex (Pi), and only occasionally were labeled cells observed in area SII dorsal to the superior limiting sulcus. Figure 7C illustrates a case containing a retrograde tracer injection in area 36c. In contrast to the case illustrated in Figure 7B, this case contained relatively few retrogradely labeled cells in area Ig and more cells in area Pi. This pattern more closely resembled the pattern of labeling seen after injections in the medial portion of area TF (Fig. 14). The insular labeling in case M-21-91 DY, which contained an injection located in area 36d, is not shown in Figure 7 but produced a distinctive pattern of labeling. The vast majority of labeled cells was observed in the parainsular cortex with relatively fewer cells observed in areas Ia, Id, and Ig.

In general, retrogradely labeled cells were observed both in deep and superficial layers of the insular cortex (Fig. 10b–d).

Cingulate and retrosplenial cortical afferents to the perirhinal cortex. Figure 8A shows a straight-line, unfolded map of the cingulate and retrosplenial cortices demonstrating the typical distribution of retrograde labeling resulting from an injection in area 36r of the perirhinal cortex (case M-3-90 FB). Shown for comparison is an unfolded, two-dimensional density map of the cingulate and retrosplenial cortices showing a prototypical distribution of retrogradely labeled cells following an injection in area TF (Fig. 8B). After retrograde tracer injections in the perirhinal cortex, low densities of retrogradely labeled cells were consistently observed throughout the ventral portion of area 24 of the cingulate cortex. Only occasionally were labeled cells observed in areas 23, 30, 29m, and 29l of the retrosplenial cortex. Scattered labeled cells were observed in both deep and superficial layers of the cingulate cortex after injection in the perirhinal cortex (Fig. 10a–e).

Parietal lobe afferents to the perirhinal cortex. The perirhinal cortex injections resulted in either few or no labeled cells in areas 7a and 7b of the posterior parietal lobe. One exception was case M-4-91 FB, which had a FB injection in the caudal portion of area 35 (Figs. 3B, 5D). This injection resulted in labeled cells scattered throughout a larger extent of areas 7a and 7b.

Summary of cortical afferents to the perirhinal cortex

Figure 9 shows unfolded, two-dimensional density maps of the temporal lobe, frontal lobe, insular cortex, cingulate cortex, and retrosplenial cortex for case M-3-90 FB, which contained an injection in area 36r. As described previously, the four density levels shown in different colors represent the same number of labeled cells per column of cortex in all four maps. By examining the different density maps from one case, the relative strengths of projections from nearly the entire cortical mantle can be more easily appreciated.

The percentages of retrogradely labeled cells observed in different cortical areas in this case are shown in Table 1. The perirhinal cortex receives the majority of its cortical input from unimodal visual areas TE and TEO (62%) and strong inputs from polymodal areas TH and TF (25%). The strong projections from unimodal visual areas, moreover, appear to be quite convergent: a similar longitudinal strip of medial area TE projects to virtually all regions of the perirhinal cortex. The perirhinal cortex receives weaker projections from the dorsal bank of the superior temporal sulcus (6%), the insular cortex (2%), orbitofrontal areas 11–13 of the frontal lobe (2%), and from area 24 of the cingulate cortex (<1%). It receives little or no input from areas in the parietal lobe. The laminar organization of these projections can be appreciated in the coronal sections in Figure 10.

In general, areas 35 and 36 receive very similar patterns of cortical inputs, though area 35 appears to receive slightly stronger inputs from the dorsal bank of the STS. Area 36d receives little unimodal visual input and stronger inputs from polymodal areas of the parahippocampal cortex and the rostral portion of the STG.

Organization of cortical afferents to the macaque monkey parahippocampal cortex

Temporal lobe afferents to the parahippocampal cortex. Because the distribution of cortical afferents to areas TF and TH of the parahippocampal cortex is substantially different from that observed for the perirhinal cortex, we have separated the description of the connections to these two areas. The overall organization of this section, however, closely parallels that just employed for the perirhinal cortex. Figure 11 consists of a series of unfolded maps of the temporal lobe illustrating the distributions and relative densities of retrogradely labeled cells in five cases in which the injections were located at different positions within areas TF and TH. Figure 12 illustrates similar maps for cases M-1-92 FB and M-1-92 DY, which contained injections that were located at, or just lateral to, the border of area TF with areas TE and TEO, respectively. Unlike the cases with injections clearly confined to area TF, these experiments exhibited a quite distinct pattern of retrograde labeling and will thus be described separately. In contrast to the relatively subtle topography observed for corticoperirhinal connections, cortical projections to area TF were organized along easily detectable mediolateral and rostrocaudal gradients. It should also be noted that, although there were few if any differences in the patterns of cortical inputs to areas 35 and 36 of the perirhinal cortex, there were some striking differences in cortical projections to areas TF and TH of the parahippocampal cortex.

Labeling in area V4. Area V4 gives rise to a moderate to strong projection to all levels of areas TF and TH. In all cases (Fig. 11A–E), it is a rather restricted region of area V4, located just caudal to the caudal boundary of area TF, that gives rise to these projections. This most rostral portion of area V4 may correspond to an area Boussaoud et al. (1991) have referred to as area VTF (see also Gattass et al., 1985). Only occasional labeled cells were observed more caudally in area V4.

Labeling in areas TE and TEO. In contrast to the high density of retrogradely labeled cells observed in areas TE and TEO after perirhinal injections, there were only moderate to low numbers of labeled cells in TE and TEO resulting from injections in area TF (Fig. 11A,C–E) and even fewer labeled cells following area TH injections (Fig. 11B). The
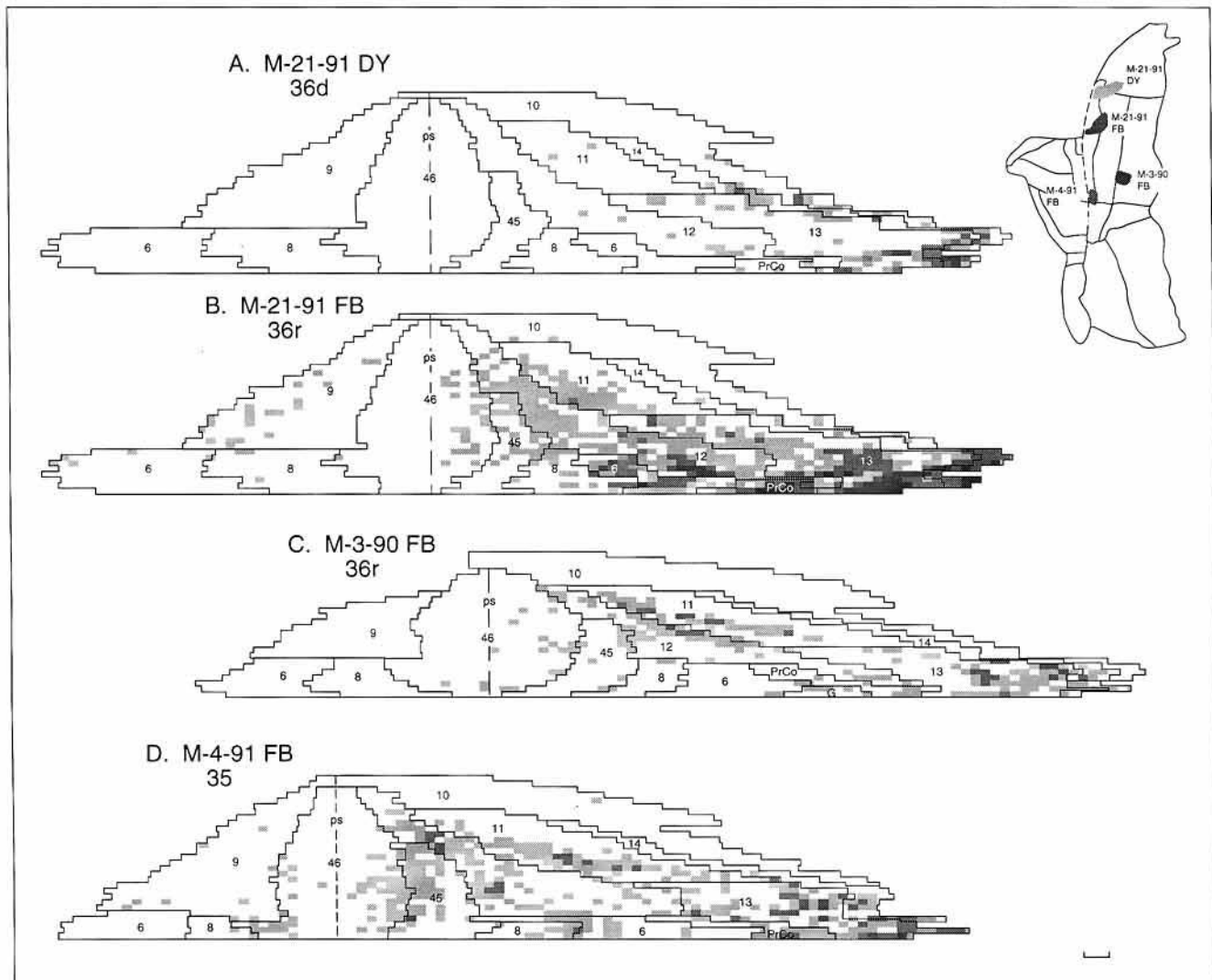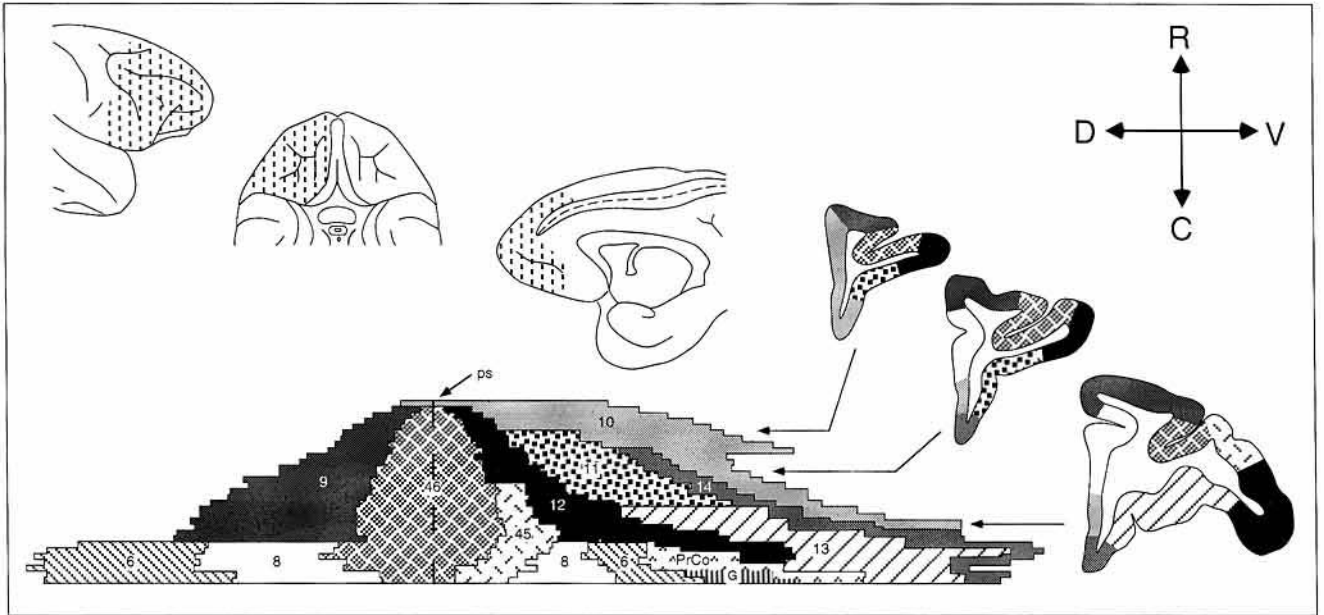
Figure 6

highest densities of labeled cells projecting to TF were consistently located in medial portion of area TEO within the banks of the occipitotemporal sulcus as well as in the caudomedial portion of area TE. The medial portions of areas TE and TEO also gave rise to the heaviest projections to the perirhinal cortex with progressively lighter projections originating from more lateral portions of areas TE and TEO. There also appeared to be a mediolateral topography, such that the more laterally placed injections in area TF (Fig. 11D,E) tended to have the highest numbers of retrogradely labeled cells in areas TE and TEO, whereas more medially situated injections (Fig. 11A,C) tended to have fewer labeled cells in these areas. The weakest projections from areas TE and TEO were observed after injections placed in area TH (Fig. 11B).

Labeling in the ventral bank of the superior temporal sulcus (STSv). Low (Fig. 11A,C) to moderate (Fig. 11D,E) densities of retrogradely labeled cells were consistently observed in the STSv after injections in area TF. The labeled cells tended to be scattered throughout approximately the rostral half of the STSv. There also appeared to be a mediolateral topography, such that the highest numbers of retrogradely labeled cells were observed in STSv after injections placed in the lateral portions of area TF (Fig. 11D,,E), whereas progressively smaller numbers of cells were observed in STSv after more medially placed injections in area TF (Fig. 11A,C). There were few labeled cells observed in the STSv after injections of area TH (Fig. 11B).

Labeling in the dorsal bank of the superior temporal sulcus (STSd). One of the strongest temporal lobe projections to area TF originated along the dorsal bank of the superior temporal sulcus (STSd). STSd labeling tended to be slightly weaker after injections confined to area TH. As with the STSd projections to the perirhinal cortex, STSd cells projecting to the parahippocampal cortex were organized in "patches." The STSd projections also exhibited mediolateral and a rostrocaudal gradients. We will first describe the mediolateral gradient by comparing two cases with injections at two different mediolateral locations of area TF. We will then consider the rostrocaudal gradient by considering cases with injections at two different rostrocaudal levels of area TF.

The mediolateral topography can be appreciated by examining Figure 11C and 11E, which illustrate cases containing injections at approximately the same rostrocaudal level but at different mediolateral positions of area TF. The more medially placed injection (Fig. 11C) resulted in the heaviest labeling in the more lateral portions of the STSd, whereas the more laterally situated injection in area TF (Fig. 11E) demonstrated a higher density of cells in the medial portions of STSd (closest to the fundus of the STS). This relationship can also be appreciated by comparison of Figure 11A and 11D. Substantial numbers of retrogradely labeled cells were observed in STSd after injections in area TH (Fig. 11B); however, the "patch"-like pattern of labeling was not as prominent in those cases. Consistent with the mediolateral organization described above, injections in TH produced the highest density of labeled cells in the most lateral portion of STSd (close to the dorsal lip of the sulcus).

The rostrocaudal topography of STSd projections to area TF can be appreciated by comparing Figure 11D, which illustrates a case containing a more rostrally situated injection in area TF, with Figure 11E, which illustrates a caudally situated injection. In both cases, the projection from STSd appeared to be coarsely focused in two patches. The location of these patches shifted depending on the rostrocaudal location of the injection site. Thus, in Figure 11D, the patches were located rostrally in STSd, and, in Figure 11E, the patches were located substantially more caudally. A similar rostrocaudal topography can be seen by comparing Figures 11A and 11C.

Labeling in the superior temporal gyrus. The cortex of the STG projects both to area TF and area TH. In general, the projection to area TH was somewhat more substantial than to area TF. There was also a mediolateral gradient to the projection, such that STG projected most heavily to area TH (Fig. 11B), somewhat less heavily to medial portions of area TF (Fig. 11A,C), and even less heavily to lateral portions of area TF (Fig. 11D,E). In no case were retrogradely labeled cells observed in the primary auditory area located more caudally on the superior temporal plane.

Labeling in the perirhinal cortex. Injections involving either area TH or area TF resulted in moderate (Fig. 11A,C–E) to low (Fig. 11B) densities of retrogradely labeled cells within the perirhinal cortex. The labeled cells were observed most commonly and in highest numbers in area 36c.

Labeling in the parahippocampal cortex. After injections in area TF, there were consistently high densities of retrogradely labeled cells in area TH (Fig. 11A,C–E). Similarly, after injections in area TH, area TF contained high densities of retrogradely labeled cells (Fig. 11B). In one representative case with a retrograde tracer injection in area TH (Fig. 11B, Table 1), 51% of all retrogradely labeled cortical cells were observed in area TF. This represented the highest percentage of labeled cells observed in any cortical area in this case. Thus, areas TH and TF are strongly interconnected.

Results of atypical cases M-1-92 FB and M-1-92 DY. Case M-1-92 DY (Fig. 12A) and M-1-92-FB (Fig. 12B) contained injections located on the border of area TF with areas TE and TEO, respectively, as determined by cytoarchitectonic criteria. The results of these cases illustrate that areas of cortex that have cytoarchitectonic characteristics transitional between one area and another also exhibit patterns of connectivity that are "transitional" between the patterns typical for both areas. Thus, both of these cases demonstrated numerous labeled cells in STSd and

---

Fig. 6. **Top:** Representative two-dimensional, unfolded map of the frontal lobe of the *Macaca fascicularis* monkey. On the top left are three different surface views of the frontal lobe. The shaded portion indicates the region that has been unfolded. To the right are three representative coronal sections wherein the shading patterns correspond to regions of the unfolded map with the same shading patterns. Arrows indicate the region of the unfolded map from which these sections were taken. In the unfolded map, the different cortical areas are labeled and shown in distinct shading patterns. The point of alignment for this map was the fundus of the principal sulcus (ps), shown as a dashed line. The compass indicates the axes of the unfolded maps in both the top and bottom, where R, C, D, and V correspond to rostral, caudal, dorsal and ventral, respectively. **Bottom (A–D):** Four representative two-dimensional, unfolded maps of the frontal lobe in cases with injections in the perirhinal cortex. The case name and injection site are indicated for each map. The density levels determined from the distribution of labeled cells in the temporal lobe were applied to the unfolded maps of the frontal lobe (see text for more details). Shown on the top right is an unfolded, two-dimensional map similar to the one shown in Figure 3 indicating the location of the retrograde tracer injection sites for these four cases. G, Gustatory cortex; PrCO, precentral opercular cortex; Areas 6, 8–14, 45, and 46 after the terminology of Walker (1940) with slight modifications as described by Carmichael (1993). Scale bar = 2 mm.
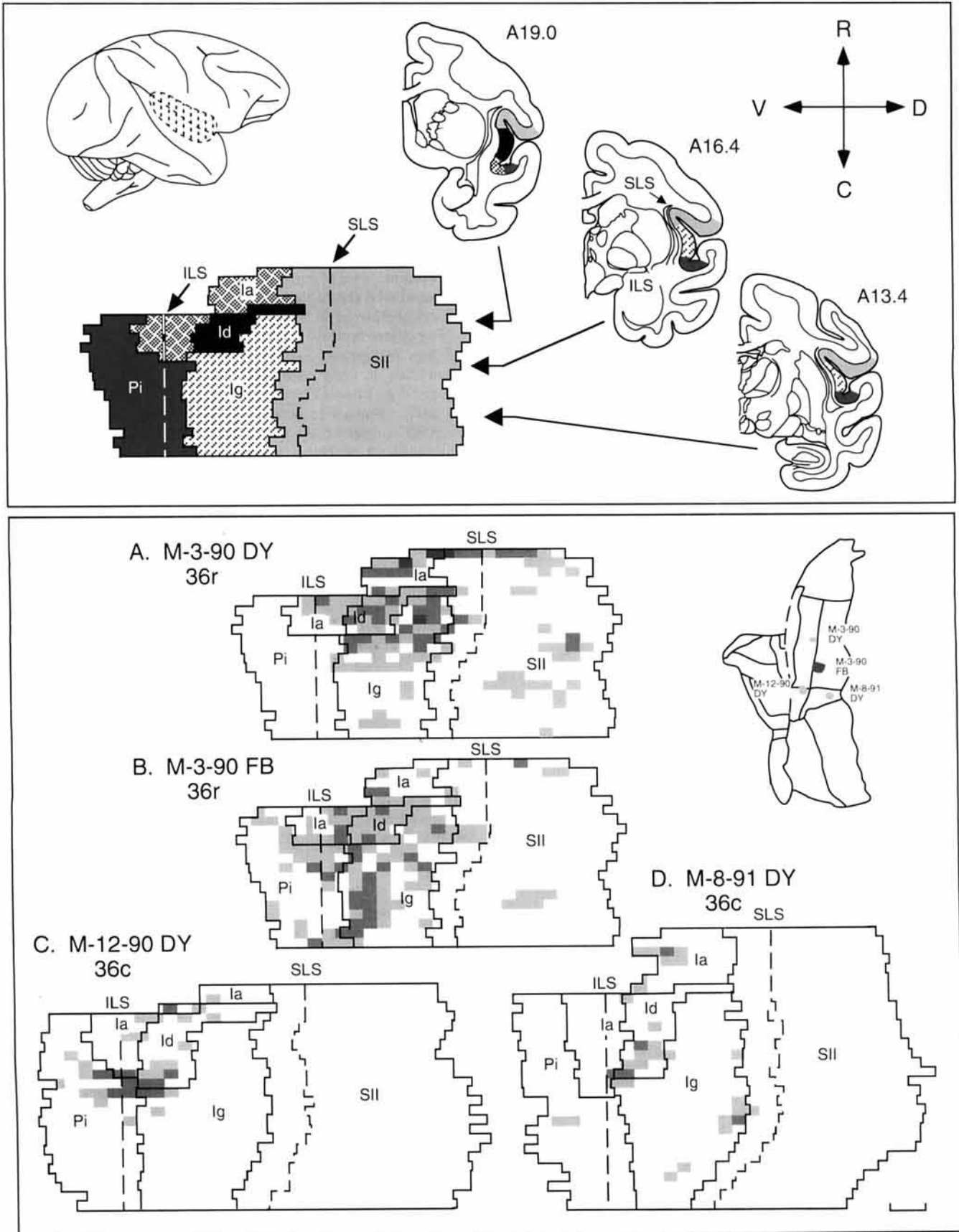
Figure 7

heavy intrinsic labeling within area TF; both of these characteristics are typical of TF injections. However, these cases also demonstrated heavy retrograde labeling throughout areas TE and TEO that is more characteristic of injections in areas TE and TEO than in area TF. Both of these border injections also produced retrograde labeling at more caudal levels of area V4 than is typical of injections confined to area TF. Thus, these cases provide strong evidence that the lateral border of area TF, as determined by cytoarchitectonic criteria, also identifies a region of changing cortical connectivity.

Laminar organization of retrogradely labeled cells in the temporal lobe. In general, retrogradely labeled cells in the temporal lobe after injections in areas TH and TF were observed primarily in layers III, V, VI, and occasionally in layer II. There appeared to be approximately equal numbers of labeled cells in deep and superficial layers (Fig. 17b–f).

Summary of temporal lobe afferents to the parahippocampal cortex

The pattern of retrograde labeling in the temporal lobe resulting from injections in the parahippocampal cortex is distinctly different from that following injections in the perirhinal cortex. The temporal lobe projections to areas TH and TF also exhibited a more easily observable mediolateral and rostrocaudal topography than the projections to the perirhinal cortex. Summarized in Table 1 are the percentages of retrogradely labeled cells observed in different portions of the temporal lobe in one representative case containing an injection in area TF and one representative case containing an injection in area TH. The strongest temporal lobe labeling after injections in area TF was observed in the caudal unimodal visual area V4 (perhaps including area VTF). In one prototypical case with an area TF injection (M-2-90 FB; Fig. 11C), 31% of the labeled cortical cells were located in area V4 (Table 1). In another case with a TH injection (M-3-91 FB; Fig. 11B), retrogradely labeled cells in area V4 accounted for 8% of the total labeled cortical cells (Table 1). Unimodal visual inputs also arose from caudomedial levels of area TE and from medial portions of area TEO. In the prototype TF injection case,

approximately 11% of the labeled cells were located in areas TE and TEO; few cells in these areas, however, appear to project to area TH (1%). Areas TF and TH receive a prominent input from the polymodal areas located on the dorsal bank of the STS (STSd). For the prototype cases described in Table 1, 17% of the labeled cells were in STSd following the TF injection, and 15% of the labeled cells were in this region following the TH injection. Perhaps the most striking difference between areas TF and TH was in the relative innervation by visual vs. auditory regions of the temporal lobe. Area TH received relatively little unimodal visual input but received relatively strong projections from auditory association cortex of the STG. Area TF, on the other hand, received substantial unimodal visual input but relatively little input from the auditory cortex.

Frontal lobe afferents to the parahippocampal cortex. Figure 13 presents a series of straight-line, unfolded density maps of the frontal lobe that illustrate the distribution of retrogradely labeled cells following injections in the parahippocampal cortex. The pattern of labeling in the frontal lobe was quite consistent across all injections in areas TF or TH. In all cases, low to moderate densities of labeled cells were observed in the midrostrocaudal levels of area 46, particularly in the area located ventral to the principal sulcus. Labeling was also consistently observed in area 9, on the dorsal surface of the frontal lobe, as well as in the caudal portion of area 13. In the cases illustrated in Figure 13A,D, small numbers of retrogradely labeled cells were also observed in the rostral portion of area 11. The injections in both of these cases, however, involved some of the white matter deep to area TF, and the labeling in area 11 may have resulted from this contamination.

Figure 17a shows a representative coronal section through the frontal lobe in case M-2-90 FB illustrating the laminar distribution of labeled cells. In general, labeled cells were observed in both deep and superficial layers, but the labeling in deep layers tended to be heavier.

Insular cortex afferents to the parahippocampal cortex. Figure 14 presents a series of unfolded density maps of the insular cortex that illustrate the distribution of retrogradely labeled cells following injections in the parahippocampal cortex. Overall, there tended to be low to moderate numbers of cells in all subdivisions of the insular cortex following parahippocampal injections. Moreover, the insular projections were organized along a mediolateral gradient, such that injections in area TH (Fig. 14D) resulted in the strongest labeling ventrally in the parainsular cortex (Pi), and injections placed at progressively more lateral positions within area TF (Fig. 14C,F,G) produced higher densities of labeled cells progressively more dorsally in the agranular, dysgranular, and granular portions of the insular cortex. The labeled cells were observed in both deep and superficial layers.

Cingulate and retrosplenial cortical afferents to the parahippocampal cortex. Injections throughout areas TH and TF produced similar patterns of labeling in the cingulate and retrosplenial cortices. Figures 8B and 16C illustrate the same unfolded density map of the cingulate and retrosplenial cortices for case M-2-90 FB. A low to moderate number of retrogradely labeled cells was observed throughout the rostral portions of areas 24 and 32. There were fewer labeled cells in the caudal part of area 24 and in area 23. By far the strongest input arose from areas 30, 291, and 29m of the retrosplenial cortex. These areas consistently contained moderate to high numbers of retrogradely la-

Fig. 7. **Top:** Representative unfolded, two-dimensional map of the insular cortex of the brain of the *Macaca fascicularis* monkey. On the top left is a lateral view of the monkey brain with the banks of the lateral sulcus "opened up" to show the location of the insular cortex. Shown to the right are three coronal sections adapted from the atlas of Szabo and Cowan (1984), where the shaded cortical areas correspond to the shading patterns in the unfolded map. Arrows indicate the approximate rostrocaudal level of the unfolded map where these sections would be located. In the unfolded map, the various cortical areas are labeled and shown in distinctive shading patterns. Dashed lines represent the fundus of the inferior limiting sulcus (ILS) or fundus of the superior limiting sulcus (SLS). The point of alignment for this map was the fundus of the inferior limiting sulcus. The compass indicates the axes of the unfolded maps in both the top and bottom. **Bottom (A–D):** Four representative two-dimensional, unfolded density maps of the insular cortex showing the distribution of labeling resulting from injections in the perirhinal cortex. The case names and injection sites are indicated for each map. The density levels determined from the distribution of labeled cells in the temporal lobe for each case have also been applied to the unfolded maps of the insular cortex (see text for details). Shown at the upper right is an unfolded, two-dimensional map showing the locations of the injection sites in these cases. Ia, agranular insula; Id, dysgranular insula; Ig, granular insula; ILS, inferior limiting sulcus; Pi, parainsular cortex; SII, second somatosensory area; SLS, superior limiting sulcus. Scale bar = 2 mm.
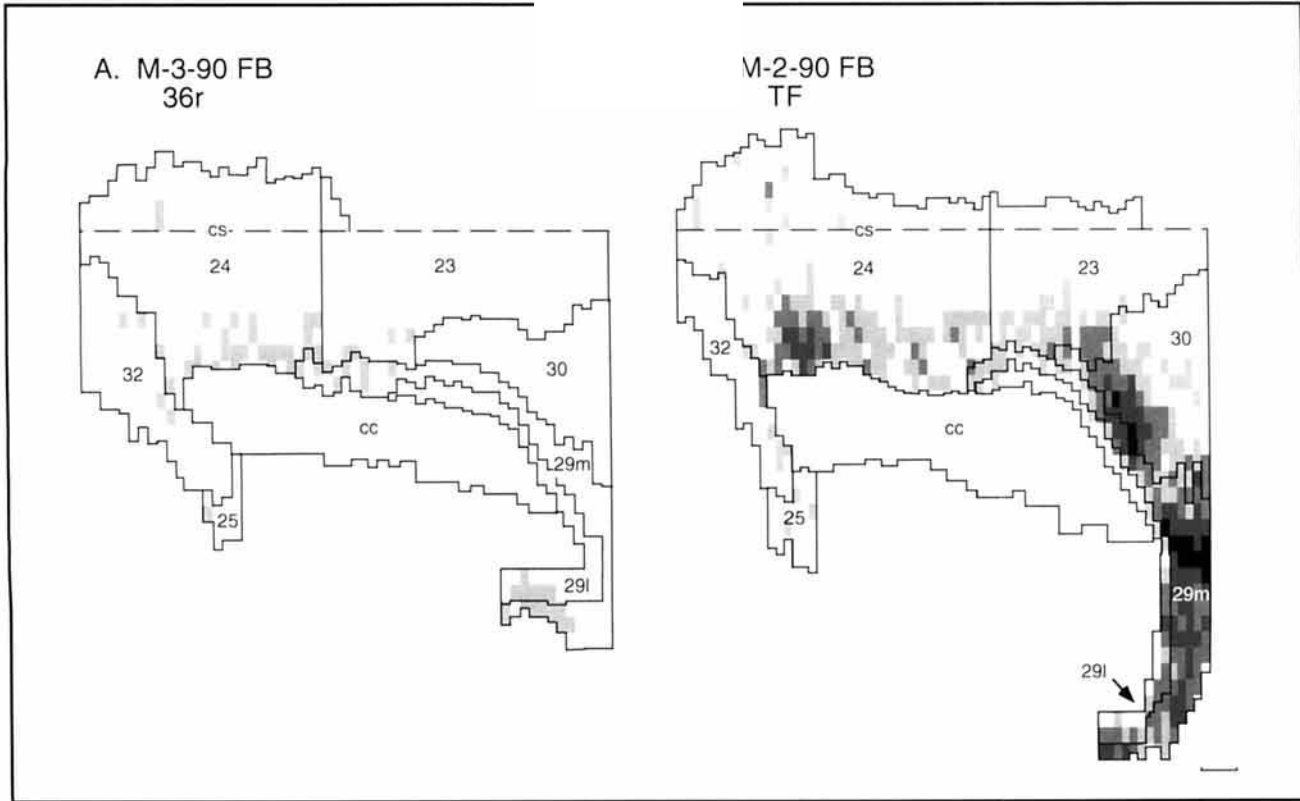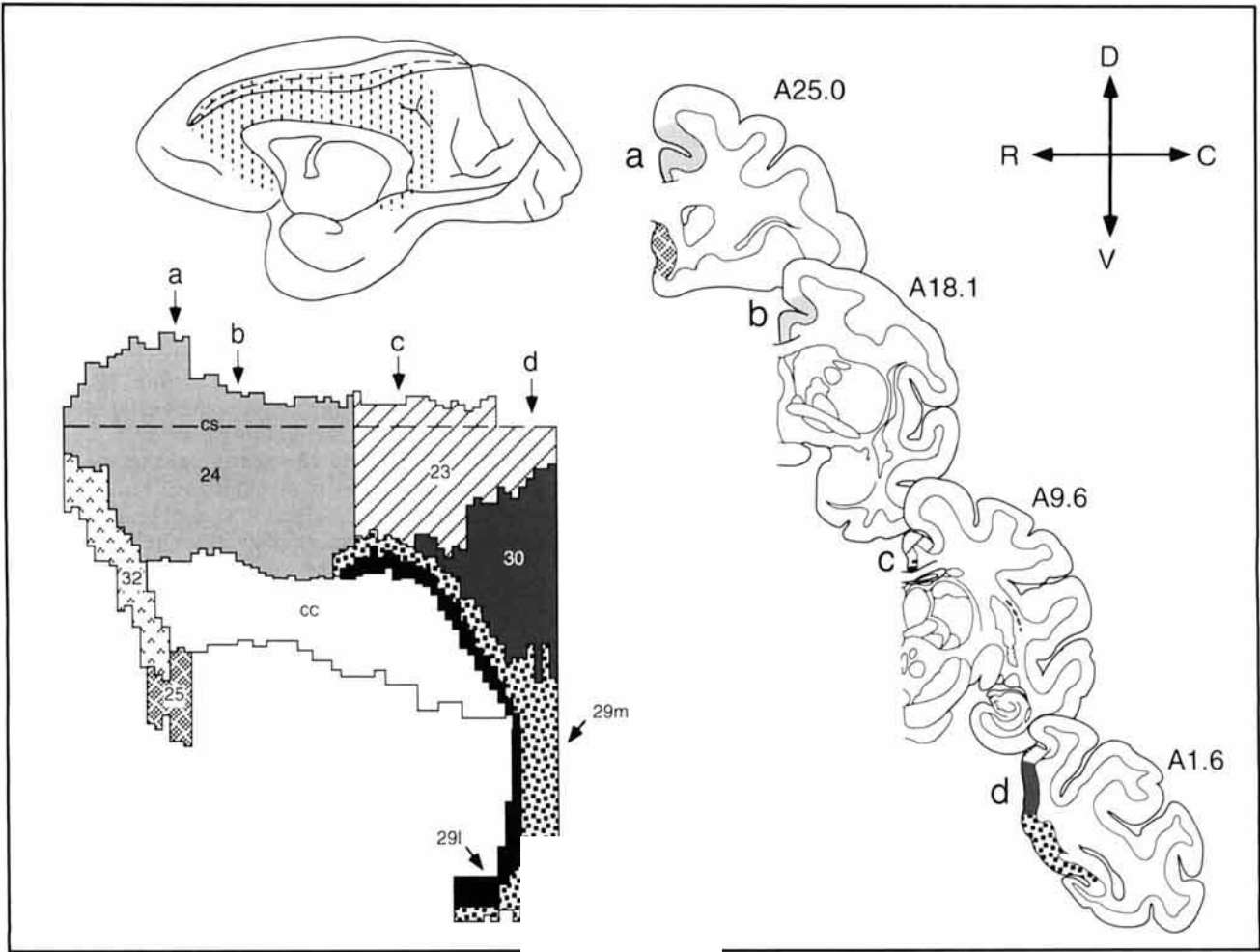
A. M-3-90 FB
36r

M-2-90 FB
TF

Figure 8

beled cells after injections in any portion of areas TH or TF. This pattern of labeling contrasts markedly with the pattern seen after injections in the perirhinal cortex (Fig. 8A) where few, if any, labeled cells were observed in the retrosplenial cortex.

Figure 17b–f illustrates the laminar distribution of retrogradely labeled cells in the cingulate and retrosplenial cortices after an injection in area TF (Case M-2-90 FB). Labeled cells were observed in both superficial and deep layers.

Parietal lobe afferents to the parahippocampal cortex. A substantial number of labeled cells was consistently observed in area 7a and area LIP of the posterior parietal lobe after injections of area TF. A few cells were also observed in area 7b. Interestingly, only small numbers of labeled cells were observed in the parietal lobe after injections in area TH. Figure 15 presents a series of coronal sections through the parietal lobe showing the typical pattern of labeling following an injection in area TF (M-2-90 FB). The density of the retrograde labeling in the parietal lobe appeared to vary depending on the mediolateral position of the area-TF injection. Injections situated laterally in area TF produced the highest density of labeled cells in area 7a and LIP; progressively more medially placed injections produced progressively lower densities of retrogradely labeled cells in these areas. Injections in area TH produced few if any labeled cells in posterior parietal cortex.

The laminar distribution of labeled cells in the posterior parietal cortex after an injection in area TF can be see in Figures 15 and 17f. In general, labeled cells were observed in both superficial and deep layers.

Summary of cortical afferents to the parahippocampal cortex

Figure 16 shows unfolded density maps for the temporal lobe, frontal lobe, insular, cingulate, and retrosplenial cortices for case M-2-90 FB, which contained an injection in area TF. The percentage of retrogradely labeled cells observed in various cortical regions in this case as well as in case M-3-91 FB, which contained an injection in area TH, are shown in Table 1. Both areas TF and TH receive prominent projections from the cingulate and retrosplenial cortex, comprising 21% and 24%, respectively, of the total number of cortical-labeled cells observed. Area TF also receives prominent inputs from visual areas V4, area TEO,

Fig. 8. **Top:** Representative unfolded, two-dimensional map of the cingulate (areas 25, 32, and 24) and retrosplenial (areas 23, 30, 29m, and 29l) cortices. Shown at top left is a view of the medial surface of the macaque monkey brain. The shaded area represents the region that has been unfolded. In the unfolded map, the different cortical areas are labeled and indicated by different shading patterns. Dashed lines represent the fundus of the cingulate sulcus (cs), which was used as the alignment point for the sections. On the right are four coronal sections adapted from the atlas of Szabo and Cowan (1984). The shading patterns in the coronal sections correspond to the shading patterns in the unfolded map. The compass indicates the axes of the unfolded maps in both the top and bottom. **Bottom:** Unfolded, two-dimensional density maps of the cingulate and retrosplenial cortices in case M-3-90 FB (**A**), which contained an injection in area 36, and case M-2-90 FB (**B**), which contained an injection in area TF. See Figure 3 for location of the injection sites. The density levels determined from the distribution of labeled cells in the temporal lobe from these cases were also applied to the cell count data from the cingulate and retrosplenial cortices (see text for details). Additional abbreviations: cc, corpus callosum. Scale bar = 2 mm.
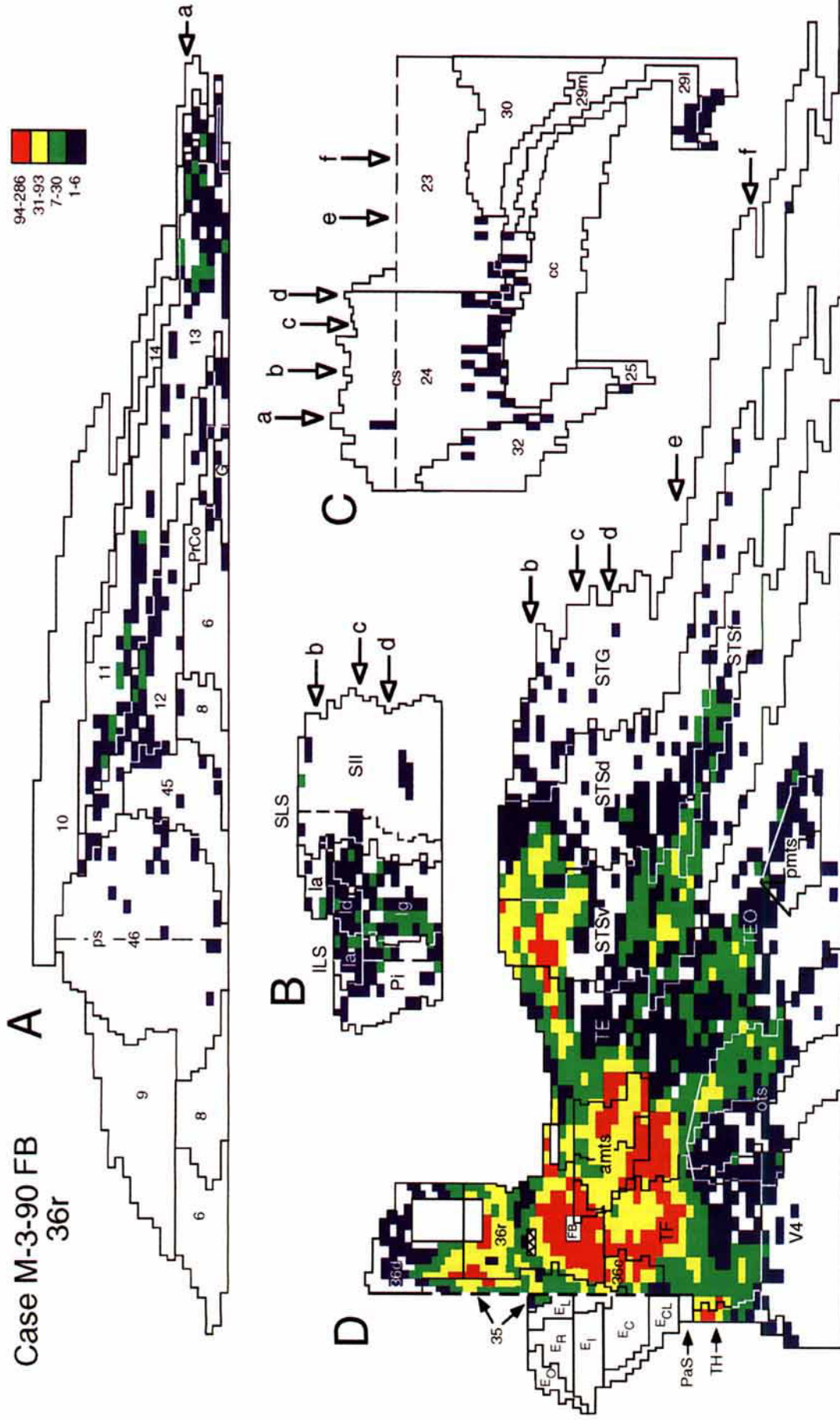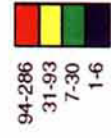
and the caudal portion of area TE, as well as a moderate projection from area 7a of the posterior parietal lobe. In contrast, area TH receives substantially less prominent input from unimodal visual areas or from posterior parietal lobe, but it receives its strongest cortical input from area TF. Area TH also appears to receive proportionately stronger inputs from the auditory association areas of the STG (9%) compared to area TF (1%).

DISCUSSION

Converging evidence from neuropsychological, neuroanatomical, and electrophysiological lines of research indicate that the perirhinal and parahippocampal cortices play a prominent role in normal memory function. In their seminal 1970 paper, Jones and Powell highlighted the unique position of the cortical regions lying adjacent to the primate rhinal sulcus as recipients of convergent sensory information. They demonstrated that the cortex of the parahippocampal gyrus, which they labeled area 35 of Brodmann (1909), and suggested was homologous to area TH of Bonin and Bailey (1947), received convergent projections from higher-order unimodal cortical regions as well as from other presumed polymodal areas, such as the dorsal bank of the superior temporal sulcus. The multimodal character of the cortex surrounding the rhinal sulcus was confirmed, in part, by early electrophysiological studies, which found that neurons in this region were responsive to stimuli presented in multiple modalities (Desimone and Gross, 1979).

Relatively little work was carried out on the perirhinal and parahippocampal cortices until the studies of Van Hoesen and Pandya (1975), who demonstrated strong projections from these areas to the entorhinal cortex. More recently, Insausti et al. (1987) used retrograde tracing techniques to determine the full scope of cortical inputs to the macaque monkey entorhinal cortex. They demonstrated that the perirhinal cortex (defined as areas 35 and 36) and the parahippocampal cortex (defined as areas TF and TH) gave rise to approximately two-thirds of the cortical inputs to the entorhinal cortex. Projections between the entorhinal cortex and the perirhinal and parahippocampal cortices have also been shown to be both reciprocal and topographically organized (Suzuki and Amaral, 1994a). Given the intriguing functional implication of the connections described above, it is somewhat surprising that there have been only meager neuroanatomical efforts to better establish the borders, subdivisions, and intrinsic and extrinsic connectivity of the perirhinal and parahippocampal cortices. Therefore, we have initiated a series of studies aimed at providing a comprehensive description of the neuroanatomy of the primate perirhinal and parahippocampal region.

In the present study, we used retrograde tracers to establish the full complement of cortical inputs to the macaque monkey perirhinal and parahippocampal cortices. Consistent with the description by Jones and Powell (1970), we found that the perirhinal and parahippocampal cortices receive inputs from both unimodal and polymodal associational areas. However, a unique contribution of the present study is the finding that the perirhinal cortex, area TF, and area TH each receive a different subset of these cortical inputs. The perirhinal cortex receives its strongest input from unimodal visual areas TE and rostral TEO as well as from polysensory areas TF and TH. Area TF, in contrast, receives its strongest visual input from the caudalmost

Fig. 9. Two-dimensional, unfolded density maps for the frontal lobe (**A**), insular cortex (**B**), cingulate and retrosplenial cortices (**C**), and temporal lobe (**D**) for case M-3-90 FB, which contained an injection in area 36r of the perirhinal cortex. At upper right is a scale indicating the number of retrogradely labeled cells per column of cortex represented by the four different colors. All other conventions are the same as shown in the previous figures. Open arrows with lower case letters indicate the rostrocaudal positions of the coronal sections illustrated in Figure 10. Scale bar = 2 mm.

Figure 10 (See legend overleaf.)

extent of area TE, area TEO, and rostral area V4. Another distinguishing feature between area TF and the perirhinal cortex is that the former receives substantial input from the retrosplenial cortex (areas 23, 29, and 30) and from polymodal areas of the dorsal bank of the superior temporal sulcus, whereas the latter does not. Area TH is unique in receiving only modest unimodal visual input and proportionately stronger innervation from the auditory associational areas of the STG. In the following sections, we compare our current findings with those from previous studies and also discuss the functional implications of our findings.

The cortical afferents of the perirhinal cortex: Comparison with previous studies and functional implications

Projections from visual areas. Jones and Powell (1970) initially reported weak projections from the lateral portion of area TE (area 21) to area 35. More recently, both Van Hoesen and Pandya (1975) and Webster et al. (1991) reported prominent inputs from areas TE and TEO to the perirhinal cortex. Similar projections have been reported in the cat (Room and Groenewegen, 1986).

We have found that the largest proportion of cortical inputs to the perirhinal cortex originates in unimodal visual areas TE, rostral portions of area TEO, and the cortex of the ventral bank of the superior temporal sulcus (STSv). One of the most striking findings of this study was that a longitudinally organized strip of cortex, primarily situated medially in areas TE and rostral TEO, projected in a highly convergent manner onto much of the perirhinal cortex. Interestingly, all portions of the perirhinal cortex give rise to a highly convergent projection to the rostrolateral entorhinal cortex (Suzuki and Amaral, 1994a). Although the detailed functional organization of areas TE and TEO is poorly understood, the fact that only medial portions of these cortical areas project to the perirhinal cortex may be the basis for functional differentiation between medial and lateral portions of areas TE and TEO. This is consistent with a variety of previous evidence that areas TE and TEO can be divided into medial and lateral (or dorsal and ventral) subdivisions (Seltzer and Pandya, 1978; Iwai, 1981; Felleman et al., 1986; Horel et al., 1987; Iwai and Yukie 1987; Yukie et al., 1988, 1990; Felleman and Van Essen, 1991; Van Essen et al., 1991; Weller and Steele, 1992).

The extensive projection from visual areas TE and TEO to the perirhinal cortex is consistent with a growing body of electrophysiological and behavioral data suggesting that the perirhinal cortex may be particularly involved in mediating certain forms of visual recognition memory. Lesions that involve the perirhinal cortex produce substantial visual object memory impairment in the macaque monkey (Murray and Mishkin, 1986; Zola-Morgan et al., 1989b; Gaffan and Murray, 1992; Meunier et al., 1993, Suzuki et al., 1993). Moreover, neurons located in and around the

perirhinal cortex exhibit memory related responses during performance of the delayed match-to-sample task (Miyashita and Chang, 1988; Miller, et al., 1991, 1993; Riches et al., 1991; Fahy et al., 1993). Interestingly, both Miller et al. (1993) and Riches et al. (1991) emphasize that the responses of cells in this region have both sensory and memory components. Thus, not only do these cells exhibit selective visual responses, but the memory of the sample stimulus appears to be carried in the modulation of the neuron's visual response throughout the delayed match-to-sample trial (Miller et al., 1993). This finding is perhaps indicative of the privileged position the perirhinal cortex occupies in the flow of information between purely visual areas (area TE) and other memory related areas (hippocampal formation).

Projections from areas TF and TH. Both Van Hoesen and Pandya (1975) and Martin-Elkins and Horel (1992) reported projections from area TF to the perirhinal cortex. In our experiment M-3-90 FB, which contained a retrograde tracer injection confined to the perirhinal cortex (Figs. 9, 10), 25% of all retrogradely labeled cells in the neocortex were observed in areas TF and TH (Table 1). The overlapping termination within the perirhinal cortex of projections from areas TE, TEO, TF, and TH allow for potential combination of visual, spatial, and auditory information (see below). We wish to emphasize that, although the perirhinal cortex receives a prominent input from the parahippocampal cortex, the reciprocal projection is relatively meager. Only area 36c provides a substantial return projection to the parahippocampal cortex. This pattern of connectivity stands in marked contrast to the organization of most corticocortical projections that are generally reciprocated (Rockland and Pandya, 1979; Suzuki and Amaral, 1994a).

Projections from insular cortex. Mesulam and Mufson (1982b) demonstrated that the insular cortex projects to the perirhinal cortex. Our data are consistent with this finding. In one prototypical case, 2% of all the direct cortical input to the perirhinal cortex arose from the insular cortex (Table 1). The granular and dysgranular portions of the insular cortex have strong connections with somatosensory association areas including area SII (Jones and Powell, 1970; Mesulam and Mufson 1982a,b; Freedman et al., 1986). Electrophysiological studies indicate that the granular portion of the insula is a unimodal somatosensory area (Schneider et al., 1993).

These findings indicate that projections from the insula provide the major route for somatosensory information to the perirhinal cortex. This projection is of particular interest, because macaque monkeys with bilateral lesions of the perirhinal and parahippocampal cortices are significantly impaired on a tactual version of the delayed nonmatching-to-sample task (Suzuki et al., 1993). The insula to perirhinal projection, however, is not the only somatosensory projection to the medial temporal lobe. Areas TH and TF also receive direct projections from all portions of the insular cortex (Table 1), and the entorhinal cortex receives a direct projection from the agranular insula that, in turn, receives projections from the dysgranular and granular portions of the insula (Insausti et al., 1987). Thus, there appear to be a number of potential direct and indirect routes by which somatosensory information can reach the medial temporal lobe. The quantitative methods used in these analyses highlight the disproportionately large visual inputs to the perirhinal cortex (62%; Table 1) relative to the somatosensory input (2%; Table 1). Although the precise

Fig. 10. (See previous page.) **a–f:** Line drawings of representative coronal sections arranged from rostral (a) to caudal (f) from case M-3-90 FB, which contained an injection in area 36r. The injection site is shown in section c. The black region represents the core of the dye injection while the white region corresponds to the zone of heavy labeling and bright fluorescence that typically surrounds the core. Black dots indicate the locations of individual retrogradely labeled cells. Cortical subdivisions and layer IV of the cortex are indicated. All abbreviations are the same as in previous figures.

relationship between the number of retrogradely labeled cells and the potential functional significance of a particular projection is not known, it would appear that the primate medial temporal lobe is predominantly influenced by the visual system.

Projections from frontal lobe. Van Hoesen et al. (1975) and Morecraft et al. (1992) found that the orbitofrontal cortex, particularly area 13, is reciprocally interconnected with the perirhinal cortex. We also found the largest number of retrogradely labeled cells in area 13 and observed smaller numbers of labeled cells in the more rostrally situated areas 11 and 12. Only occasionally were labeled cells observed in dorsal and dorsolateral areas 6, 8, 9, or 46.

Although the overall number of retrogradely labeled cells in the frontal lobe following perirhinal injections was rather low (Table 1, Case M-3-90 FB), it may provide the substrate for the relay of memory-related information from the frontal lobe to the medial temporal lobe. Wilson et al. (1993) recently presented evidence for a dissociation of spatial and object processing domains in the primate prefrontal cortex. Cells in the inferior convexity (including areas 11 and 12) were more responsive to visual stimuli used in a pattern delayed-response task than to cues used during a spatial delayed-response task. Conversely, cells of the dorsolateral prefrontal cortex (area 46) had the reverse pattern of responsivity. Thus, areas in the prefrontal cortex involved in visual object working memory (areas 11 and 12) project to the perirhinal cortex, whereas those involved in spatial working memory (area 46) do not.

The cortical afferents of areas TF and TH of the parahippocampal cortex: Comparison with previous studies and functional implications

Projections from visual areas. Although the parahippocampal cortex receives a prominent input from the visual system, this arises from more caudally situated visual areas than those that project to the perirhinal cortex. The visual inputs to the parahippocampal cortex originate in rostral portions of area V4, medial portions of area TEO, and caudomedial portions of area TE. A number of studies in the macaque monkey have reported that area V4 projects to area TF (Rockland and Pandya, 1979; Rosene and Pandya, 1983; Felleman et al., 1986; Blatt et al., 1989; Boussaoud et al., 1991; Barnes and Pandya, 1992). Projections to TF have also been observed from the apparent homologue of V4 of macaque monkeys, the dorsolateral area of owl and squirrel monkeys (Weller and Kaas, 1987; Steele et al., 1991a). What was not clear from these earlier studies, however, was the magnitude of these visual inputs to area TF. We found that the rostral V4 projection constituted the single largest cortical input to area TF. Following retrograde tracer injections in area TF, the number of labeled cells in area V4 was highest in a relatively small rostrocaudal region of cortex situated just caudal to the caudal boundary of area TF. This area may correspond to area VTF (a caudal, visually responsive area of TF) of Boussaoud et al. (1991), also referred to as area VF of Gattass et al. (1985). Boussaoud et al. (1991) reported that area VTF contains a representation of the central visual field. In contrast to area TF, area TH receives a relatively smaller projection from visual areas. However, the strongest projection originates from the same anteriorly situated portion of area V4 (possibly area VTF) that projects heavily to area TF.

Another visual input to area TF arose in area TEO and the caudal portions of area TE (Pandya and Kuypers, 1969;

Seltzer and Pandya, 1976; Rockland and Pandya, 1979; Rosene and Pandya, 1983; Felleman et al., 1986; Blatt et al., 1989; Boussaoud et al., 1991; Barnes and Pandya, 1992; Distler et al., 1993). As with the TE and TEO projections to the perirhinal cortex, it was only the medial portions of area TEO and caudal TE that projected to area TF. This finding is consistent with the studies of Webster et al. (1991), who reported no projections from lateral portions of areas TE and TEO to the parahippocampal cortex, and with the report of Distler et al. (1993), who reported projections from the medial portions of area TEO to area TF. Moreover, Distler et al. (1993) demonstrated that, whereas the laterally situated foveal representation of TEO does not project to area TF, the medially situated peripheral representation of TEO does project to areas TF and TH.

Projections from retrosplenial and cingulate cortices. Both Baleydier and Mauguiere (1980) and Pandya et al. (1981) reported projections from the retrosplenial cortex to areas TH and TF of the parahippocampal cortex. The present study has not only confirmed this projection, but the quantitative analyses indicated that the retrosplenial cortex provides the second largest projection to areas TH and TF (Table 1). Areas TH and TF also receive projections from more rostral portions of the cingulate cortex, but these projections were considerably less dense than the projections arising from the retrosplenial cortex.

Neuroanatomical studies in the macaque monkey (Vogt and Pandya, 1987) and the cat (Olson and Musil, 1992a) indicate that the retrosplenial cortex receives input from visual, auditory, somatosensory, and polymodal associational areas. Consistent with these neuroanatomical findings, electrophysiological studies in the cat (Olson and Musil, 1992b) have demonstrated that retrosplenial neurons are responsive to stimuli in a number of different modalities and also have responses related to eye movements. A particularly prominent input to the retrosplenial cortex arises in the posterior parietal cortex (Vogt and Pandya, 1987; Cavada and Goldman-Rakic, 1989; Andersen et al., 1990), an area known to be involved in visuospatial function (see below).

Behavioral studies indicate that the retrosplenial cortex may contribute to the control of spatially guided behavior. In the rat, lesions of the cingulate and retrosplenial cortices (Markowska et al., 1989) or lesions limited to the retrosplenial cortex (Sutherland et al., 1988) produce a significant deficit on tasks of spatial memory. The prominent projection from the retrosplenial cortex to areas TH and TF provides a route by which spatial information can influence the medial temporal lobe. This, however, is not the only potential route. The retrosplenial cortex also has a prominent direct projection to the caudal half of the entorhinal cortex (Insausti et al., 1987), the same region to which the parahippocampal cortex projects (Suzuki and Amaral, 1994a). Thus, putative spatial information from the retrosplenial cortex can reach the hippocampal formation either directly, via the retrosplenial projection to the entorhinal cortex, or indirectly, via the projection to the parahippocampal cortex.

Posterior parietal cortex. The projections from the posterior parietal lobe to area TF of the parahippocampal cortex in the macaque monkey has been well established (Pandya and Kuypers, 1969; Jones and Powell, 1970; Seltzer and Pandya, 1976, 1984; Mesulam et al., 1977; Cavada and Goldman-Rakic, 1989; Andersen et al., 1990; Blatt et al., 1990). Our quantitative analysis has shown that, although the posterior parietal cortex provides a
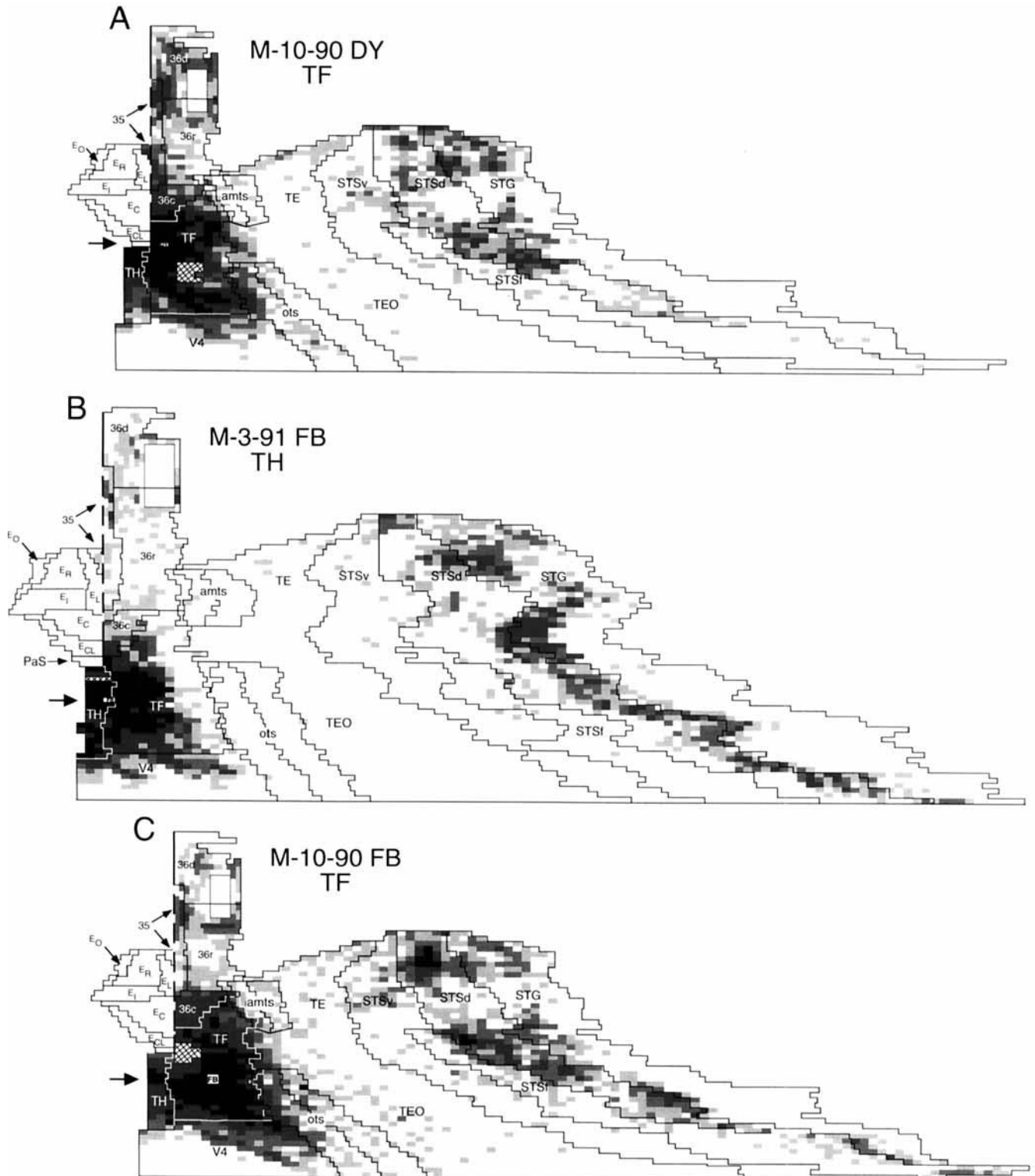
Fig. 11. **A–E:** Two-dimensional, unfolded density maps of the temporal lobe of five representative cases with retrograde tracer injections located throughout areas TH and TF. The position of the unfolded maps on these facing pages corresponds to the relative rostrocaudal or mediolateral location of their injection site within the parahippocampal cortex. See Figure 3 for an illustration of the relative location of these injection sites. Case names and injection sites are indicated for each map. The location of the injection sites for the individual cases are shown in white and are marked with either "FB," to indicate a fast-blue injection, or "DY," to indicate a diamidino-yellow injection. The rostrocaudal location of the injection in each case is indicated by a large black arrow to the left of the maps. The cross-hatched area represents the location of the other injection site that precluded analysis of retrogradely labeled cells. The white, rectangular area in the temporal pole of each map represents a region of cortex (i.e., the tip of the temporal pole) that could not be unfolded, because coronal sections through this region are cut obliquely, and layer IV is not visible. As in previous figures, black voxels represent regions containing the highest density of retrogradely labeled cells, whereas progressively lighter shades of gray represent progressively lower densities of labeling. Scale bar = 3.5 mm.
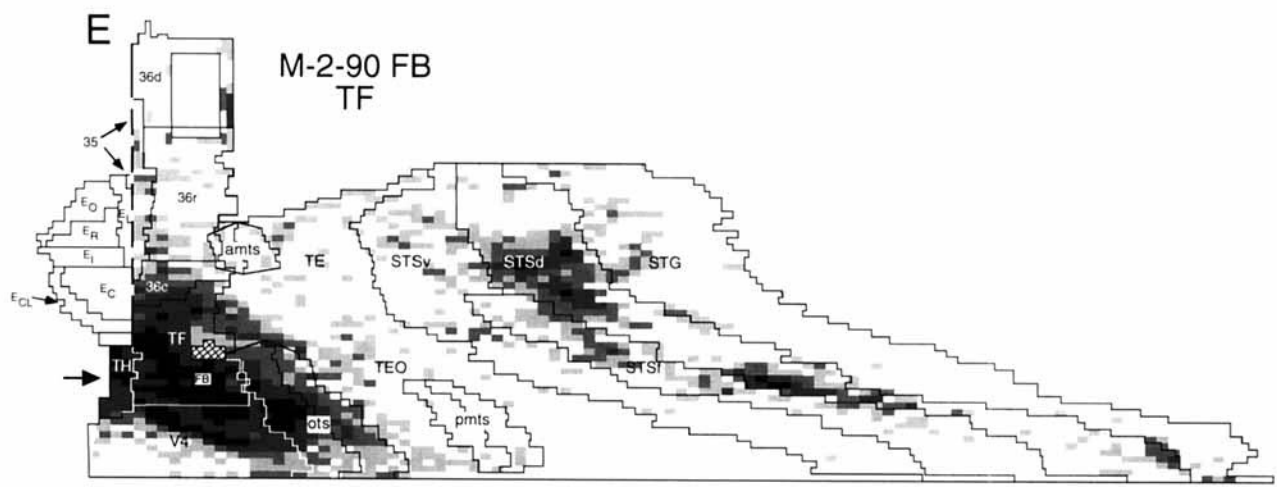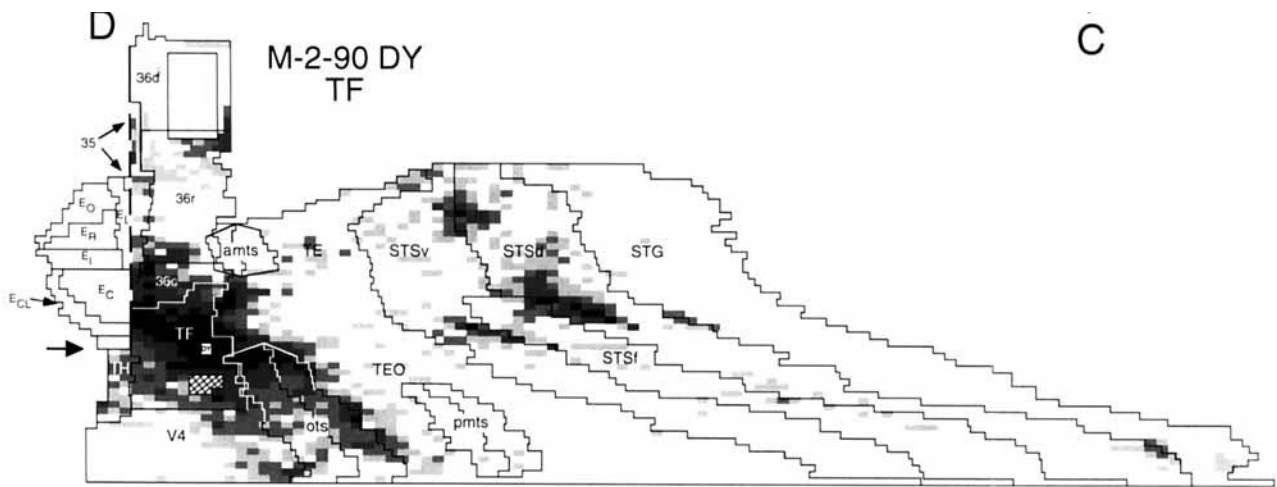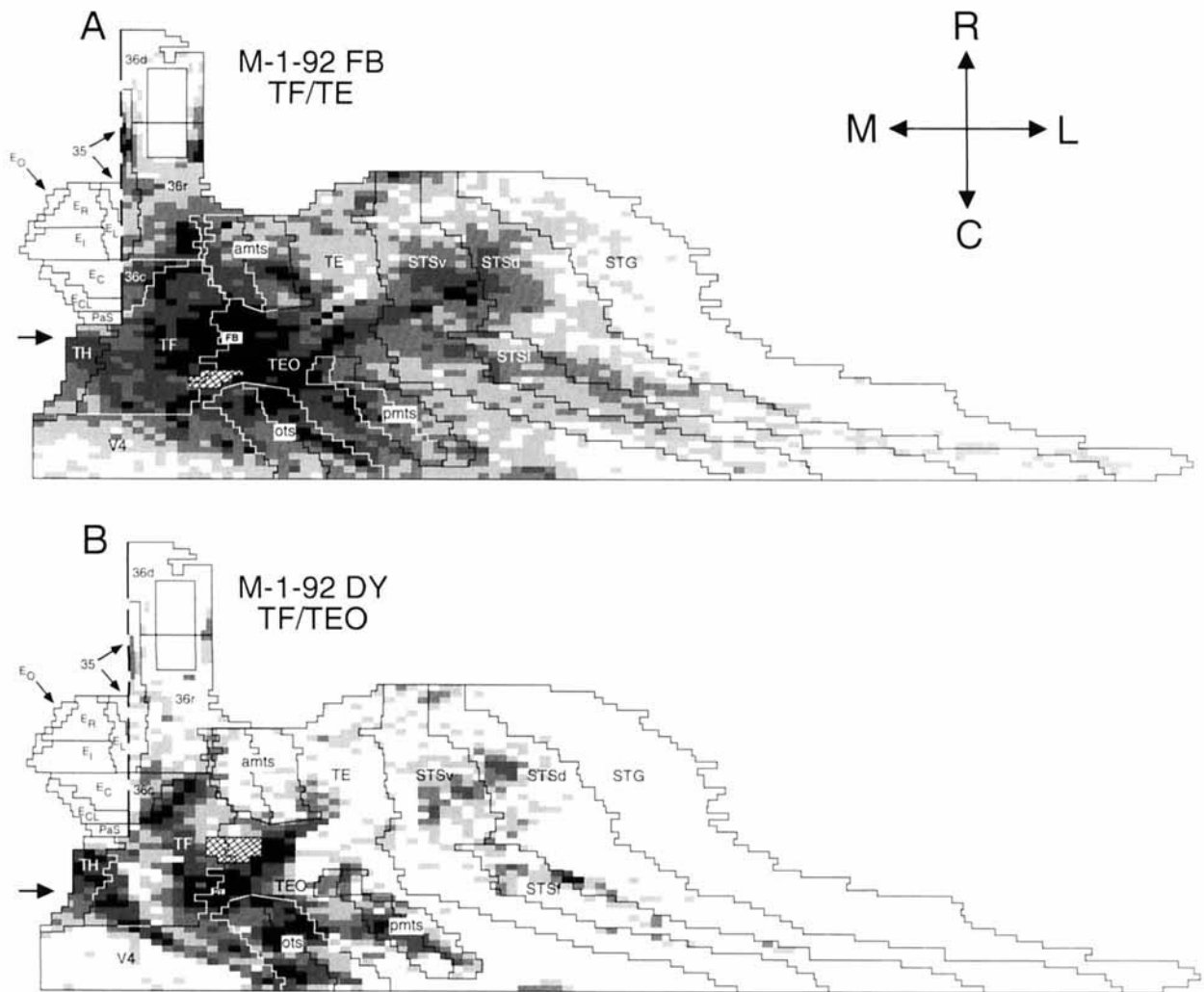
Figure 11.   continued

Fig. 12. **A,B:** Two-dimensional, unfolded density maps of the temporal lobe in cases M-1-92 FB and case M-1-92 DY, which contained injections that were located at the lateral border of area TF with areas TE and TEO, respectively. All conventions are the same as in Figure 11. Scale bar = 3.5 mm.

TABLE 1. Percentage of Cortical Retrogradely Labeled Cells

Area	Injection in area 36 (M-3-90 FB)	Injection in area TF (M-2-90 FB)	Injection in area TH (M-3-91 FB)
Temporal lobe	95	67	74
Area 35/36	—	4	3
Area TH	1	5	—
Area TF	24	—	51
Area TE/TEO	62	11	<1
Area V4	2	30	3
Area STSd	6	16	8
Area STG	<1	1	9
Frontal lobe	2	3	1
Insular cortex	2	1	1
Cing. and Retrospl. cortex	<1	21	24
Post. Parietal cortex	<0.1	8	<0.001

moderate projection to area TF (in one representative case, 9% of all the cortical input to area TF originated in posterior parietal cortex; Table 1), it provides essentially no

input to area TH (<0.001% in one representative case; Table 1).

Electrophysiological studies support the idea that the parietal cortex is involved in the processing of visuospatial information (Andersen, 1989). Case studies in humans and experimental studies in macaque monkeys indicate that damage to the parietal cortex produces deficits in visuospatial perception tasks such as reaching tasks (Ettlinger and Wegener, 1958; Bates and Ettlinger, 1960), landmark tasks (Pohl, 1973; Milner et al., 1977; Ungerleider and Brody, 1977; Brody and Pribram, 1978), route-following tasks (Petrides and Iversen, 1979), stylus-maze tasks (Milner et al., 1977), and cage finding (Sugishita et al., 1978). The direct projection from posterior parietal cortex to area TF provides another possible route by which visuospatial information may reach the medial temporal lobe.

Dorsal bank of the superior temporal sulcus (STSd). The cortex lining the dorsal bank of the superior temporal sulcus (STSd) is made up of a number of cytoarchitectoni-

A. M-10-90 DY
TF

B. M-2-90 DY
TF

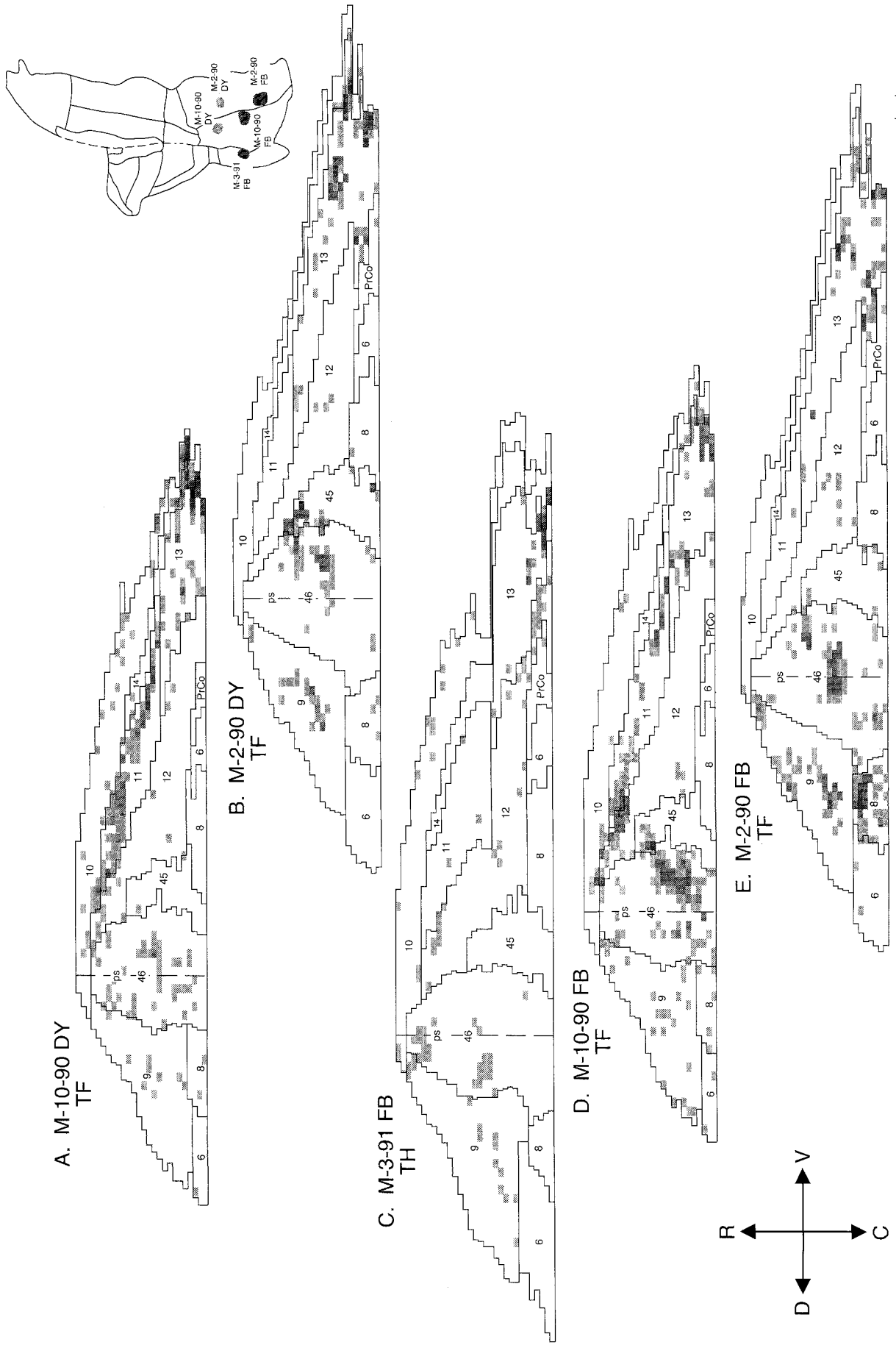C. M-3-91 FB
TH

D. M-10-90 FB
TF

E. M-2-90 FB
TF

Fig. 13. **A–E:** Five representative two-dimensional, unfolded density maps of the frontal lobe demonstrating the distribution of retrogradely labeled cells in cases with injections throughout the parahippocampal cortex. Case names and injection sites are indicated adjacent to each map. At the upper right is an unfolded, two-dimensional map showing the locations of the injection sites for these cases. All conventions are the same as in Figure 7. Scale bar = 2 mm.
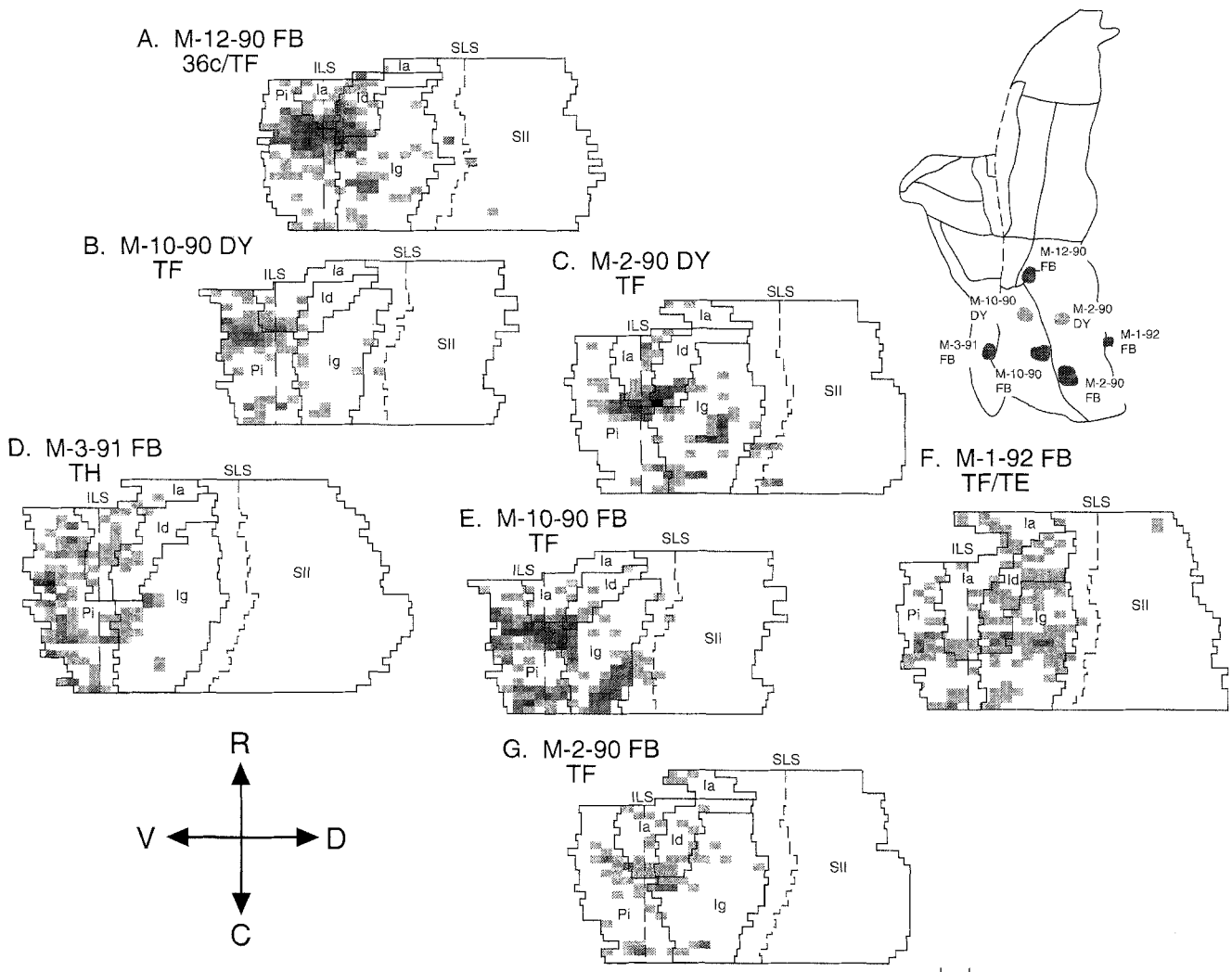
A. M-12-90 FB
36c/TF

B. M-10-90 DY
TF

C. M-2-90 DY
TF

D. M-3-91 FB
TH

E. M-10-90 FB
TF

F. M-1-92 FB
TF/TE

G. M-2-90 FB
TF

R

V ◄─────► D

C

Fig. 14. **A–G:** Seven representative two-dimensional, unfolded density maps of the insular cortex showing the distribution of retrogradely labeled cells resulting from injections throughout the parahippocampal cortex. Case names and injection sites are indicated adjacent to each map. At the upper right is an unfolded, two-dimensional map showing the locations of the injection sites for these cases. All conventions are the same as in Figure 8. Scale bar = 2 mm.

cally and connectionally distinct regions that are largely polymodal in nature (Seltzer and Pandya, 1978; Bruce et al., 1981). Bruce et al. (1981) found that 21% the cells recorded in this region responded to visual and auditory stimuli, 17% responded to visual and somesthetic stimuli, 17% were trimodal, and 41% were exclusively visual. Neuroanatomical studies have confirmed that the STSd receives convergent information from visual (Seltzer and Pandya, 1978), auditory (Seltzer and Pandya, 1978), as well as somatosensory (Mesulam and Mufson, 1982b) association areas. Barnes and Pandya (1992) showed that the STSd projects strongly to area TF. Our studies have confirmed the strong projection to area TF and provided new evidence that area TH also receives a moderate projections from STSd. In one prototypical case, 16% of retrogradely labeled cortical cells were found in STSd after an injection in area TF, and 8% of the labeled cells were located in STSd after an injection into area TH (Table 1).

There have been relatively few behavioral lesion studies examining the function of the STSd. Petrides and Iversen (1979) showed that bilateral lesions of the STSd produced a significant deficit on a route-following task. However, the deficit was not as severe as one resulting from lesions of the posterior parietal cortex. It is likely that the strong projections from the posterior parietal cortex directly to the STSd may be mediating some of these visuospatial functions.

Superior temporal gyrus. The cortex of the STG has mainly been studied in relation to auditory function (Pandya and Sanides, 1973; Seltzer and Pandya, 1978). Primary auditory cortex and unimodal auditory association cortex occupy approximately the caudal half of the STG. Although it is clear that the caudal half of the STG is involved in auditory function, the role of the rostral half of the STG remains uncertain. Recent electrophysiological studies (Baylis et al., 1987) indicate that cells in the rostral STG,
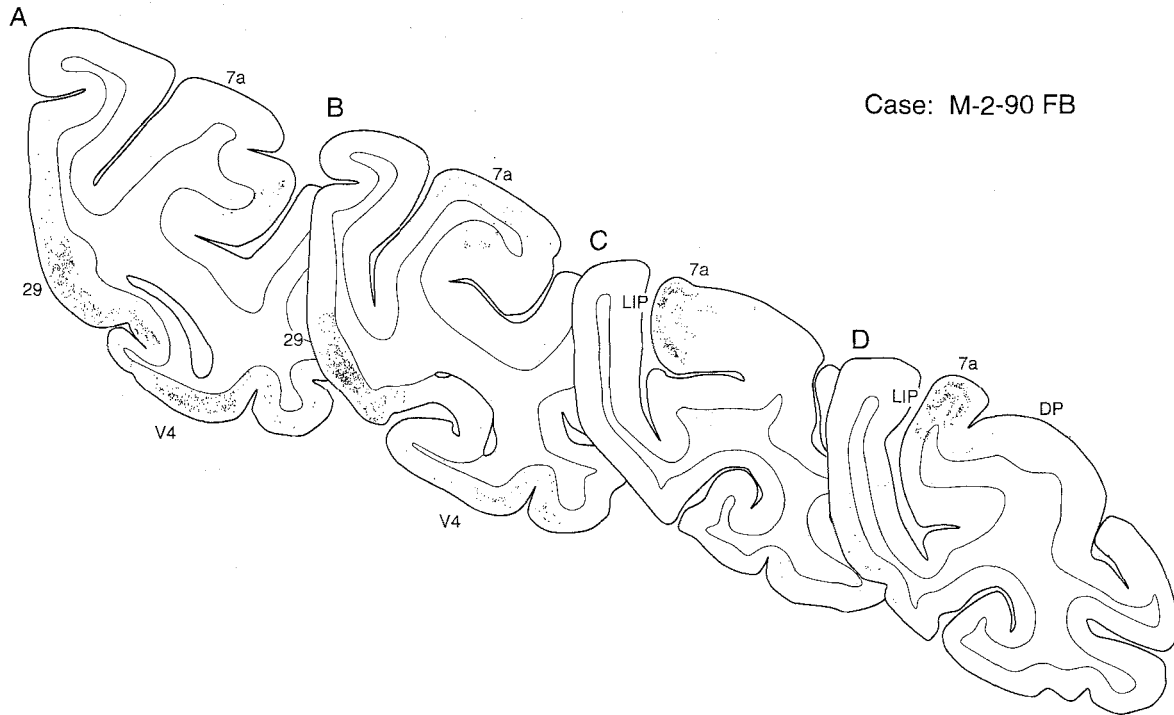
Fig. 15. **A–D:** Line drawings of representative coronal sections arranged from rostral (A) to caudal (D) through the posterior parietal lobe showing the distribution of retrogradely labeled cells in case M-2-90 FB, which contained an injection in area TF. Black dots indicate the position of individual retrogradely labeled cells.

although strongly responsive to auditory stimuli, are also responsive to visual stimuli. Thus, the rostral STG may be considered a polysensory associational area.

Tranel et al. (1988) previously reported projections from area TH to auditory association area TPT on the STG. The reverse projection, however, was not examined. We found weak-to-moderate densities of retrogradely labeled cells confined to rostromedial portions of the STG after injections in area TF. A slightly larger mediolateral and rostrocaudal extent of the STG projects to area TH. Although the STG projection to area TF constituted a relatively small proportion of its cortical input, the STG projection to area TH was its third largest input. Labeled cells were never observed in primary auditory cortex.

Frontal lobe. The dorsolateral portion of the prefrontal cortex (area 46 or the cortex of the principal sulcus) is reciprocally interconnected with the parahippocampal cortex (Pandya, et al., 1971; Goldman-Rakic et al., 1984; Barbas and Mesulam, 1985, Figs. 5, 7; Selemon and Goldman-Rakic, 1988). While Pandya and Kuypers (1969) reported projections from the orbitofrontal cortex to area TH of the parahippocampal cortex, Van Hoesen et al. (1975) failed to observe degenerating fibers in the parahippocampal cortex after lesions of the orbitofrontal cortex. In the present study, the highest numbers of retrogradely labeled cells were observed in area 46 of the principal sulcus and the caudal portion of area 13 following injections of areas TF and TH. Fewer labeled cells were observed in areas 8, 9, 11, and 45.

GENERAL SUMMARY

The quantitative neuroanatomical data presented in this study have provided a framework for understanding the flow of cortical sensory information into and through the medial temporal lobe. Figure 18 summarizes the connectivity of the macaque monkey perirhinal cortex, parahippocampal cortex, and hippocampal formation. This figure makes two major points: first, there are major differences in the organization of cortical inputs to the macaque monkey perirhinal and parahippocampal cortices. Second, from an anatomical perspective, the perirhinal and parahippocampal cortices form an interface for communication between widespread areas of the neocortex, on the one hand, and the entorhinal cortex, on the other. It is via the perirhinal and parahippocampal cortex that much of the unimodal and polymodal sensory input reaches the hippocampal formation.

Importantly, the data presented in this report also provide insight into the contributions these medial temporal lobe areas may make to memory function. For example, the strong visual inputs to the perirhinal cortex suggest that this area may be particularly involved in visual recognition memory. Consistent with this idea, Meunier et al. (1993) have shown that bilateral lesions limited to the perirhinal cortex in the macaque monkey produce a significant visual recognition memory deficit on the delayed nonmatching-to-sample task. In contrast, the strong inputs from retrosplenial cortex to areas TH and TF and the direct projections from posterior parietal cortex to area TF suggest that the
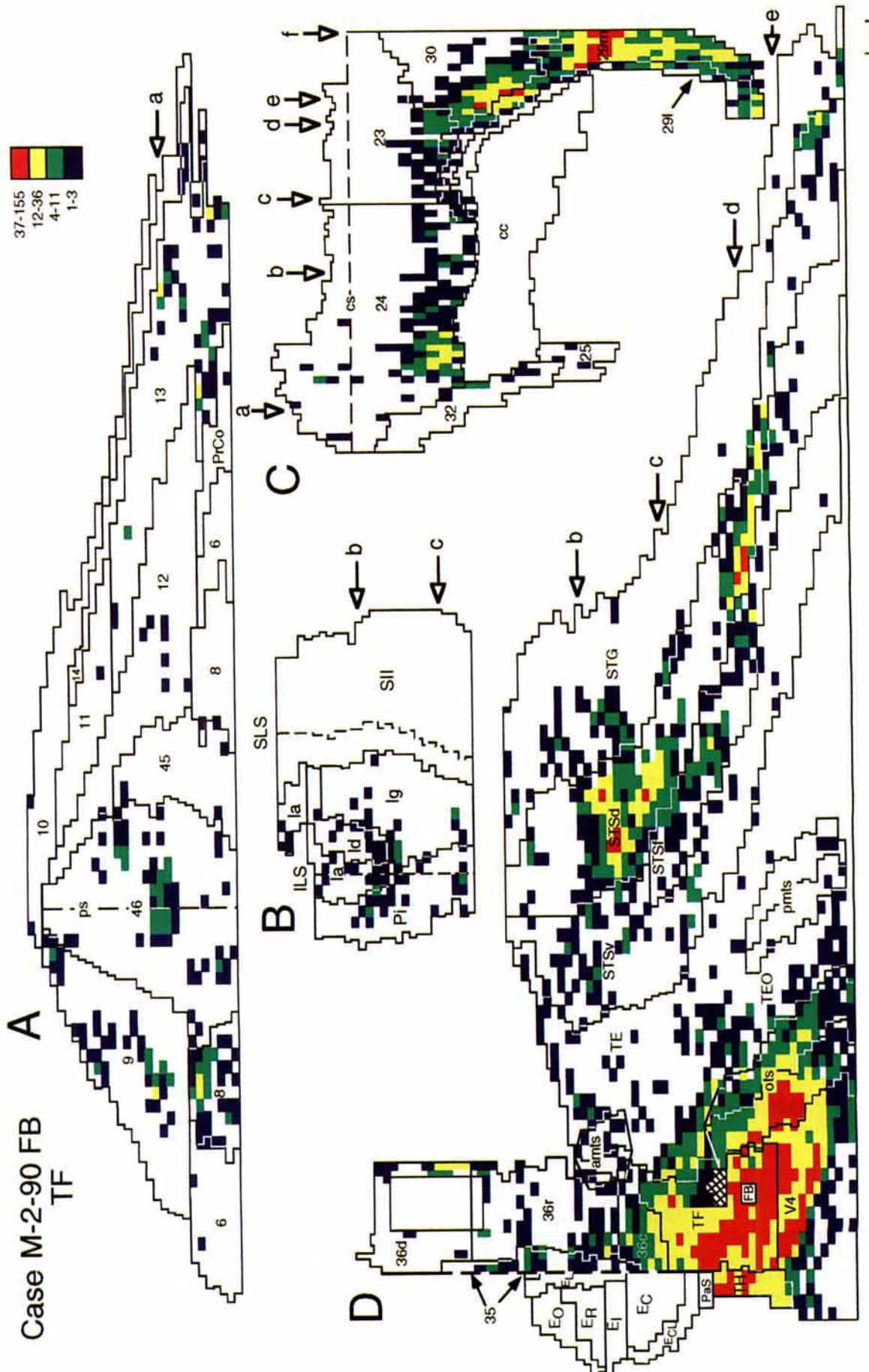
Fig. 16. Two-dimensional, unfolded density maps for the frontal lobe (**A**), insular cortex (**B**), cingulate and retrosplenial cortices (**C**), and temporal lobe (**D**) for case M-2-90 FB, which contained an injection in area TF. At upper right is a scale indicating the number of retrogradely labeled cells per column of cortex represented by the four different colors. All other conventions are the same as shown in the previous figures. Open arrows with lower case letters indicate the rostrocaudal positions of the coronal sections illustrated in Figure 17. Scale bar = 2 mm.

Fig. 17. **a–f:** Line drawings of representative coronal sections arranged from rostral (a) to caudal (f) in case M-2-90 FB, which contained an injection in area TF. The location of the injection site is shown in d. The black region represents the core of the dye injection while the white region corresponds to the zone of heavy labeling and bright fluorescence that typically surrounds the core. Each black dot represents an individual retrogradely labeled cell. Cortical subdivisions and layer IV of the cortex are indicated. All abbreviations are the same as in previous figures.
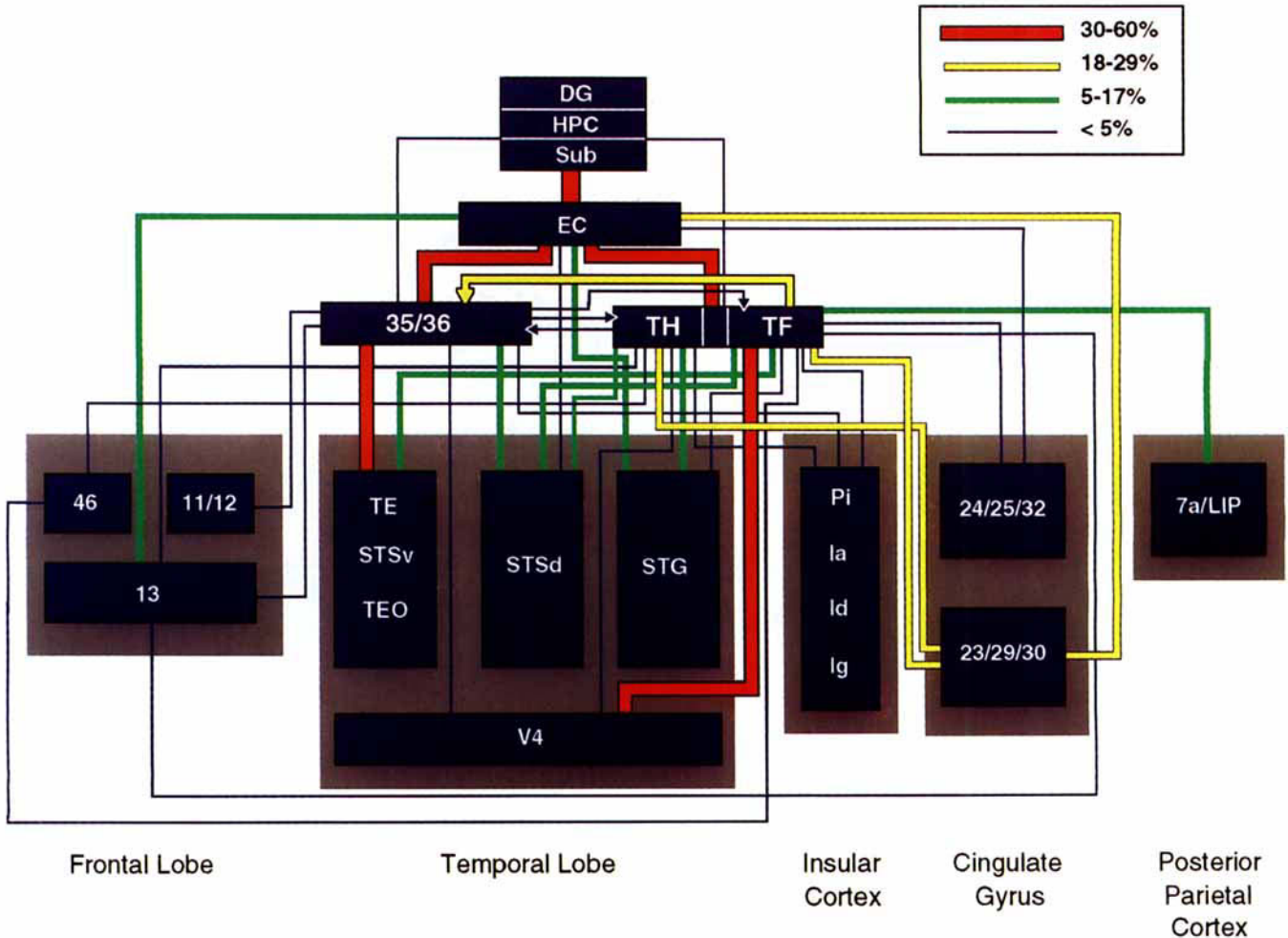
Fig. 18. "Circuit" diagram illustrating the organization and strength of cortical inputs to the entorhinal, perirhinal (area 35/36), and parahippocampal (areas TF and TH) cortices. The thick red lines represent projections providing 30–60% of the cortical input to these areas. Yellow lines represent projections providing between 18% and 29% of the cortical inputs to these areas. Green lines represent projections providing between 5% and 17% of the cortical input, and the thin blue lines represent projections providing less than 5% of the cortical input to these areas. All quantitative data were taken from Table 1 and from Insausti et al., 1987. DG, dentate gyrus; HPC, hippocampus; LIP, lateral intraparietal area; Sub, subicular complex.

parahippocampal cortex may be particularly involved in spatial memory function. Consistent with this idea is the finding in macaque monkeys that bilateral lesions of the hippocampal formation and parahippocampal cortex produce a significant deficit on a spatial memory task (Parkinson et al., 1988; Angeli et al., 1993). In humans, damage involving the parahippocampal gyrus has been reported to produce a syndrome of topographic disorientation (Habib and Sirigu, 1987). The projections from the insular cortex to both the perirhinal and parahippocampal cortices suggest that both areas may contribute to somatosensory memory function. The relatively strong projection from auditory association areas of the STG to area TH suggests that this area may be particularly involved in auditory memory function. In conclusion, our findings have not only provided a quantitative analysis of the full scope of cortical inputs to the macaque monkey perirhinal and parahippocampal cortices, but these findings have also generated a series of testable predictions concerning the roles of the perirhinal and parahippocampal cortices in memory function. It will be important to address these anatomically based predictions with selective lesion studies as well as with electrophysiological techniques.

ACKNOWLEDGMENTS

LITERATURE CITED

Amaral, D.G., and J.L. Price (1983) An air pressure system for the injection of tracer substances into the brain. J. Neurosci. Methods 9:35–43.

Amaral, D.G., R. Insausti, and W.M. Cowan (1987) The entorhinal cortex of the monkey: I. Cytoarchitectonic organization. J. Comp. Neurol. 264:326–355.

Andersen, R.A. (1989) Visual and eye movement functions of the posterior parietal cortex. Annu. Rev. Neurosci. 12:377–403.

Andersen, R.A., C. Asanuma, G. Essick, and R.M. Siegel (1990) Corticocortical connections of anatomically and physiologically defined subdivisions within the inferior parietal lobule. J. Comp. Neurol. 296:65–113.

Angeli, S.J., E.A. Murray, and M. Mishkin (1993) Hippocampectomized monkeys can remember one place but not two. Neuropsychologia 31:1021–1030.

Baleydier, C., and F. Mauguiere (1980) The duality of the cingulate gyrus in monkey. Neuroanatomical study and functional hypothesis. Brain 103:525–554.

Barbas, H., and M.M. Mesulam (1985) Cortical afferent input to the principalis region of the rhesus monkey. Neuroscience 15:619–637.

Barnes, C.L., and D.N. Pandya (1992) Efferent cortical connections of multimodal cortex of the superior temporal sulcus in the rhesus monkey. J. Comp. Neurol. 318:222–224.

Bates, J.A.V., and G. Ettlinger (1960) Posterior biparietal ablations in the monkey. Arch. Neurol. 3:177–192.

Baylis, G.C., E.T. Rolls, and C.M. Leonard (1987) Functional subdivisions of the temporal lobe neocortex. J. Neurosci. 7:330–342.

Blatt, G.J., D.L. Rosene, and D.N. Pandya (1989) Cortical afferents to the posterior parahippocampal gyrus of the rhesus monkey. I. Input from limbic, multimodal and unimodal areas in temporal, insular, parietal and occipital cortices. Soc. Neurosci. Abstr. 15:141.

Blatt, G.J., R.A. Andersen, and G.R. Stoner (1990) Visual receptive field organization and cortico-cortical connections of the lateral intraparietal area (area LIP) in the macaque. J. Comp. Neurol. 299:421–445.

Bonin, G. von, and P. Bailey (1947) The Neocortex of Macaca Mulatta. Urbana, IL: University of Illinois Press.

Boussaoud, D., R. Desimone, and L.G. Ungerleider (1991) Visual topography of area TEO in the macaque. J. Comp. Neurol. 306:554–575.

Brodmann, K. (1909) Vergleichende Lokalisationslehre der Grosshirnrinde. Leipzig: Barth.

Brody, B.A., and K.H. Pribram (1978) The role of frontal and parietal cortex in cognitive processing: Tests of spatial and sequence functions. Brain 101:607–633.

Bruce, C., R. Desimone, and C.G. Gross (1981) Visual properties of neurons in a polysensory area in superior temporal sulcus of the macaque. J. Neurophysiol. 46:369–384.

Carmichael, S.T. (1993) The orbital and medial prefrontal cortex of the macaque: Anatomical parcellation and evidence for sensory, limbic and premotor integration. Doctoral Dissertation, Washington University, St. Louis.

Cavada, C., and P.S. Goldman-Rakic (1989) Posterior parietal cortex in rhesus monkey: I. Parcellation of areas based on distinctive limbic and sensory corticocortical connections. J. Comp. Neurol. 287:393–421.

Corkin, S. (1984) Lasting consequences of bilateral medial temporal lobectomy: Clinical course and experimental findings in H.M. Semin. Neurol. 4:249–259.

Desimone, R., and C.G. Gross (1979) Visual areas in the temporal cortex of the macaque. Brain Res. 178:363–380.

Desimone, R., and L.G. Ungerleider (1989) Neural mechanisms of visual processing in monkeys. In F. Boller and J. Grafman (eds): Handbook of Neuropsychology, Vol. 2. New York: Elsevier, pp. 267–299.

Distler, C., D. Boussaoud, R. Desimone, and L.G. Ungerleider (1993) Cortical connections of inferior temporal area TEO in macaque monkeys. J. Comp. Neurol. 334:125–150.

Ettlinger, G., and J. Wegener (1958) Somaesthetic alternation, discrimination, and orientation after frontal and parietal lesions in monkeys. Q. J. Exp. Psychol. 10:177–186.

Fahy, F.L., I.P. Riches, and M.W. Brown (1993) Neuronal activity related to visual recognition memory: Long-term memory and the encoding of recency and familiarity information in the primate anterior and medial inferior temporal and rhinal cortex. Exp. Brain Res. 96:457–472.

Felleman, D.J., and D.C. Van Essen (1991) Distributed hierarchical processing in the primate cerebral cortex. Cereb. Cortex 1:1–47.

Felleman, D.J., J.J. Knierim, and D.C. Van Essen (1986) Multiple topographic and nontopographic subdivisions of the temporal lobe revealed by the connections of area V4 in macaques. Soc. Neurosci. Abstr. 12:1182.

Freedman, D.P., E.A. Murray, J.B. O'Neill, and M. Mishkin (1986) Cortical connections of the somatosensory fields of the lateral sulcus of macaques: Evidence for a corticolimbic pathway for touch. J. Comp. Neurol. 252:323–347.

Gaffan, D., and E.A. Murray (1992) Monkeys (Macaca fascicularis) with rhinal cortex ablations succeed in object discrimination learning despite 24-hour intertrial intervals and fail at matching to sample despite double sample presentation. Behav. Neurosci. 106:30–38.

Gattass, R., A.P.B. Sousa, and E. Covey (1985) Cortical visual areas of the macaque: Possible substrates for pattern recognition mechanisms. In C. Chagas, R. Gattass, and C. Gross (eds): Pattern Recognition Mechanisms. Vatican City: Pontificae Academiae Scientiarum Scripta Varia No. 54, pp. 1–20.

Goldman-Rakic, P.S., L.D. Selemon, and M.L. Schwartz (1984) Dual pathways connecting the dorsolateral prefrontal cortex with the hippocampal formation and parahippocampal cortex in the rhesus monkey. Neuroscience 12:719–743.

Habib, M., and A. Sirigu (1987) Pure topographical disorientation: A definition and anatomical basis. Cortex 23:73–85.

Horel, J.A., D.E. Pytko-Joiner, M.L. Voytko, and K. Salsbury (1987) The performance of visual tasks while segments of the inferotemporal cortex are suppressed by cold. Behav. Brain Res. 23:29–42.

Huisman, A.M., H.G.J.M. Kuypers, F. Conde, and K. Keizer (1983) Collaterals of rubrospinal neurons to the cerebellum in rat. A retrograde fluorescent double labeling study. Brain Res. 264:181–196.

Insausti, R., D.G. Amaral, and W.M. Cowan (1987) The entorhinal cortex of the monkey: II. Cortical afferents. J. Comp. Neurol. 264:356–395.

Iwai, E. (1981) Visual mechanisms in the temporal and prestriate association cortices of the monkey. Adv. Physiol. Sci. 17:279–286.

Iwai, E., and M. Yukie (1987) Amygdalofugal and amygdalopetal connections with modality-specific visual cortical areas in macaques (Macaca fuscata, M. mulatta, and M. fascicularis). J. Comp. Neurol. 261:362–387.

Jarrard, L.E. (1993) On the role of the hippocampus in learning and memory in the rat. Behav. Neural Biol. 60:9–26.

Jones, E.G., and H. Burton (1976) Areal differences in the laminar distribution of thalamic afferents in cortical fields of the insular, parietal and temporal regions of the primates. J. Comp. Neurol. 168:197–248.

Jones, E.G., and T.P.S. Powell (1970) An anatomical study of converging sensory pathways within the cerebral cortex of the monkey. Brain 93:793–820.

Kuypers, H.G.J.M. (1984) Fluorescent neuronal tracers. Adv. Cell Neurobiol. 5:307–340.

Markowska, A.L., D.S. Olton, E.A. Murray, and D. Gaffan (1989) A comparative analysis of the role of fornix and cingulate cortex in memory: Rats. Exp. Brain Res. 74:187–201.

Martin-Elkins, C.L., and J.A. Horel (1992) Cortical afferents to behaviorally defined regions of the inferior temporal and parahippocampal gyri as demonstrated by WGA-HRP. J. Comp. Neurol. 321:177–192.

Merzenich, M.M., and J.F. Brugge (1973) Representation of the cochlear partition on the superior temporal plane of the macaque monkey. Brain Res. 50:275–296.

Mesulam, M.M., and E.J. Mufson (1982a) Insula of the old world monkey. II: Afferent cortical input and comments on the claustrum. J. Comp. Neurol. 212:23–37.

Mesulam, M.M., and E.J. Mufson (1982b) Insula of the old world monkey. III: Efferent cortical output and comments on function. J. Comp. Neurol. 212:38–52.

Mesulam, M.M., G.W. Van Hoesen, D.N. Pandya, and N. Geschwind (1977) Limbic and sensory connections of the inferior parietal lobule (area PG) in the rhesus monkey: A study with a new method for horseradish peroxidase histochemistry. Brain Res. 136:393–414.

Meunier, M., J. Bachevalier, M. Mishkin, and E.A. Murray (1993) Effects on visual recognition of combined and separate ablations of the entorhinal and perirhinal cortex in rhesus monkeys. J. Neurosci. 13:5418–5432.

Miller, E.K., L. Lin, and R. Desimone (1991) A neural mechanism for working and recognition memory in inferior temporal cortex. Science 254:1377–1379.

Miller, E.K., L. Li, and R. Desimone (1993) Activity of neurons in anterior inferior temporal cortex during a short-term memory task. J. Neurosci. 13:1460–1478.

Milner, B., S. Corkin, and H.L. Teuber (1968) Further analysis of the hippocampal amnesic syndrome: 14 year follow-up study of H.M. Neuropsychologia 6:215–234.

Milner, A.D., E.M. Ockleford, and W. Dewar (1977) Visuo-spatial performance following posterior parietal and lateral frontal lesions in stumptail macaques. Cortex 13:350–360.

Mishkin, M. (1978) Memory in monkeys severely impaired by combined but not separate removal of the amygdala and hippocampus. Nature 273:297–298.

Miyashita, Y., and H.S. Chang (1988) Neuronal correlate of pictorial short-term memory in the primate temporal cortex. Nature. 331:68–70.

Morecraft, R.J. C. Geula, and M.M. Mesulam (1992) Cytoarchitecture and neural afferents of orbitofrontal cortex in the brain. J. Comp. Neurol. 323:341–358.

Morris, R.G.M, P. Garrud, J.N.P. Rawlins, and J. O'Keefe (1982) Place navigation impaired in rats with hippocampal lesions. Nature 297:681–683.

Mumby, D.G., and J.P.J. Pinel (1994) Rhinal cortex lesions and object recognition in rats. Behav. Neurosci. 108:11–18.

Murray, E.A., and M. Mishkin (1986) Visual recognition in monkeys following rhinal cortical ablations combined with either amygdalectomy or hippocampectomy. J. Neurosci. 6:1991–2003.

Olson, C.R., and S.Y. Musil (1992a) Topographic organization of cortical and subcortical projections to posterior cingulate cortex in the cat: Evidence for somatic, ocular, and complex subregions. J. Comp. Neurol. 324:237–260.

Olson, C.R., and S.Y. Musil (1992b) Posterior cingulate cortex: Sensory and oculomotor properties of single neurons in behaving cat. Cereb. Cortex 2:485–502.

Otto, T., and H. Eichenbaum (1992) Complimentary roles of the orbital prefrontal cortex and the perirhinal-entorhinal cortices in an odor-guided delayed-nonmatching-to-sample task. Behav. Neurosci. 106:763–776.

Pandya, D.N., and H.G.J.M. Kuypers (1969) Cortico-cortical connections in the rhesus monkey. Brain Res. 13:13–36.

Pandya, D.N., and F. Sanides (1973) Architectonic parcellation of the temporal operculum in rhesus monkey and its projection pattern. Z. Anat. Entwick. Gesch. 139:127–161.

Pandya, D.N., M. Hallett, and S.K. Mukherjee (1969) Intra- and interhemispheric connections of the neocortical auditory system in the rhesus monkey. Brain Res. 14:49–65.

Pandya, D.N., P. Dye, and N. Butters (1971) Efferent cortico-cortical projections of the prefrontal cortex in the rhesus monkey. Brain Res. 31:35–46.

Pandya, D.N., G.W. Van Hoesen, and M.M. Mesulam (1981) Efferent connections of the cingulate gyrus in the rhesus monkey. Exp. Brain Res. 42:319–330.

Parkinson, J.K., E.A. Murray, and M. Mishkin (1988) A selective mnemonic role for the hippocampus in monkeys: Memory for the location of objects. J. Neurosci. 8:4159–4167.

Petrides, M., and S.D. Iversen (1979) Restricted posterior parietal lesions in the rhesus monkey and performance on visuospatial tasks. Brain Res. 161:63–77.

Pohl, W. (1973) Dissociation of spatial discrimination deficits following frontal and parietal lesions in monkeys. J. Comp. Physiol. Psychol. 82:227–239.

Riches, I.P., F.A.W. Wilson, and M.W. Brown (1991) The effects of visual stimulation and memory on neurons of the hippocampal formation and the neighboring parahippocampal gyrus and inferior temporal cortex of the primate. J. Neurosci. 11:1763–1779.

Rockland, K.S., and D.N. Pandya (1979) Laminar origins and terminations of cortical connections of the occipital lobe in the rhesus monkey. Brain Res. 179:3–20.

Room, P., and H.J. Groenewegen (1986) Connections of the parahippocampal cortex. I. Cortical Afferents. J. Comp. Neurol. 251:415–450.

Rosene D.L., and D.N. Pandya (1983) Architectonics and connections of the posterior parahippocampal gyrus in the rhesus monkey. Soc. Neurosci. Abstr. 9:222.

Schneider, R.J., D.P. Friedman, and M. Mishkin (1993) A modality-specific somatosensory area within the insula of the rhesus monkey. Brain Res. 621:116–120.

Scoville, W.B., and B. Milner (1957) Loss of recent memory after bilateral hippocampal lesions. J. Neurol. Neurosurg. Psychiatr. 20:11–21.

Selemon, L.S., and P.S. Goldman-Rakic (1988) Common cortical and subcortical targets of the dorsolateral prefrontal and posterior parietal cortices in the rhesus monkey: Evidence for a distributed neural network subserving spatially guided behavior. J. Neurosci. 8:4049–4068.

Seltzer, B., and D.N. Pandya (1976) Some cortical projections to the parahippocampal area in the rhesus monkey. Exp. Neurol. 50:146–160.

Seltzer, B., and D.N. Pandya (1978) Afferent cortical connections and architectonics of the superior temporal sulcus and surrounding cortex in the rhesus monkey. Brain Res. 149:1–24.

Seltzer, B., and D.N. Pandya (1984) Further observations on parieto-temporal connections in the rhesus monkey. Exp. Brain Res. 55:301–312.

Steele, G.E., R.E. Weller, and C.G. Cusick (1991a) Cortical connections of the caudal subdivision of the dorsolateral area (V4) in monkeys. J. Comp. Neurol. 306:495–520.

Sugishita, M., G. Ettlinger, and R.M. Ridley (1978) Disturbance of cage-finding in the monkey. Cortex 14:431–438.

Sutherland, R.J., I.Q. Whishaw, and B. Kolb (1988) Contributions of cingulate cortex to two forms of spatial learning and memory. J. Neurosci. 8:1863–1872.

Suzuki, W.A., and D.G. Amaral (1994a) Topographic organization of the reciprocal connections between the monkey entorhinal cortex and the perirhinal and parahippocampal cortices. J. Neurosci. 14:1856–1877.

Suzuki, W.A., and D.G. Amaral (1994b) The construction of straight line unfolded two-dimensional density maps of neuroanatomical projections in the monkey cerebral cortex. Submitted for publication.

Suzuki, W.A., S. Zola-Morgan, L.R. Squire, and D.G. Amaral (1993) Lesions of the perirhinal and parahippocampal cortices in the monkey produce long-lasting memory impairment in the visual and tactual modalities. J. Neurosci. 13:2430–2451.

Szabo, J., and W.M. Cowan (1984) A stereotaxic atlas of the brain of the cynomolgus monkey (Macaca fascicularis). J. Comp. Neurol. 222:265–300.

Tranel D., D.R. Brady, G.W. Van Hoesen, and A.R. Damasio (1988) Parahippocampal projections to posterior auditory association cortex (area Tpt) in old-world monkeys. Exp. Brain Res. 70:406–416.

Ungerleider L.G., and B.A. Brody (1977) Extrapersonal spatial orientation: The role of posterior parietal, anterior frontal, and inferotemporal cortex. Exp. Neurol. 56:265–280.

Van Essen, D.C., and J.H.R. Maunsell (1980) Two-dimensional maps of the cerebral cortex. J. Comp. Neurol. 191:225–281.

Van Essen, D.C., D.F. Felleman, E.A. DeYoe, J. Olavarria, and J.J. Knierim (1990) Modular and hierarchical organization of extrastriate visual cortex in the macaque monkey. Cold Spring Harbor Symp. Quant. Biol., Vol. 55. Cold Spring Harbor: Cold Spring Harbor Press, pp. 679–696.

Van Hoesen, G.W., and D.N. Pandya (1975) Some connections of the entorhinal (area 28) and perirhinal (area 35) cortices of the rhesus monkey. I. Temporal lobe afferents. Brain Res. 95:1–24.

Van Hoesen, G.W., D.N. Pandya, and N. Butters (1975) Some connections of the entorhinal (area 28) and perirhinal (area 35) cortices of the rhesus monkey. II. Frontal lobe afferents. Brain Res. 95:25–38.

Victor, M., and D. Agamanolis (1990) Amnesia due to lesions confined to the hippocampus: A clinical-pathologic study. J. Cogn. Neurosci. 2:246–257.

Vogt, B.A. (1985) Cingulate Cortex. In A. Peters and E.G. Jones (eds): Cerebral Cortex, Vol. 4: Association and Auditory Cortices. New York: Plenum Press, pp. 89–150.

Vogt, B.A., and D. N. Pandya (1987) Cingulate cortex in rhesus monkey. II. Cortical afferents. J. Comp. Neurol. 262:271–289

Walker, E.A. (1940) A cytoarchitectural study of the prefrontal area of the macaque monkey. J. Comp. Neurol. 73:59–86.

Webster, M.J., L.G. Ungerleider, and J. Bachevalier (1991) Connections of inferior temporal areas TE and TEO with medial temporal-lobe structures in infant and adult monkeys. J. Neurosci. 11:1095–1116.

Weller, R.E., and J.H. Kaas (1987) Subdivisions and connections of inferior temporal cortex in owl monkeys. J. Comp. Neurol. 256:137–172.

Weller, R.E., and G.E. Steele (1992) Cortical connections of subdivisions of inferior temporal cortex in squirrel monkeys. J. Comp. Neurol. 324:37–66.

Wilson, F.A.W., S.P. O'Scalaidhe, and P.S. Goldman-Rakic (1993) Dissociation of object and spatial processing domains in primate prefrontal cortex. Science 260:1955–1958.

Yukie, M., T. Niida, H. Suyama, and E. Iwai (1988) Interaction of visual cortical areas with the hippocampus in monkeys. Neuroscience 14:297–302.

Yukie, M., H. Takeuchi, Y. Hasegawa, and E. Iwai (1990) Differential connectivity of inferotemporal area TE with the amygdala and the hippocampus in the monkey. In E. Iwai and M. Mishkin (eds): Vision, Memory and Temporal Lobe. New York: Elsevier Science Publishing Co., pp. 129–135.

Zeki, S.M. (1971) Cortical projections from two prestriate areas in the monkey. Brain Res. 34:19–35.

Zola-Morgan, S., and L.R. Squire (1986) Memory impairment in monkeys following lesions of the hippocampus. Behav. Neurosci. 100:165–170.
Zola-Morgan, S., and L.R. Squire (1993) Neuroanatomy of memory. Annu. Rev. Neurosci. 16:547–563.

Zola-Morgan, S., L.R. Squire, and D.G. Amaral (1986) Human amnesia and the medial temporal region: Enduring memory impairment following a bilateral lesion limited to field CA1 of the hippocampus. J. Neurosci. 6:2950–2967.

Zola-Morgan S., L.R. Squire, and D.G. Amaral (1989a) Lesions of the amygdala that spare adjacent cortical regions do not impair memory or exacerbate the impairment following lesions of the hippocampal formation. J. Neurosci. 9:1922–1936.

Zola-Morgan, S., L.R. Squire, D.G. Amaral, and W.A. Suzuki (1989b) Lesions of perirhinal and parahippocampal cortex that spare the amygdala and hippocampal formation produce severe memory impairment. J. Neurosci. 9:4355–4370.